CAPITAL UNIVERSITY OF SCIENCE AND TECHNOLOGY, ISLAMABAD

Back-EMF Estimation of Sensorless Brushless DC Motor Using Sliding Mode Observer

by

Attabik Tabib

A thesis submitted in partial fulfillment for the degree of Master of Science

in the

Faculty of Engineering
Department of Electrical Engineering

2022

This research is dedicated to my family

CERTIFICATE OF APPROVAL

Back-EMF Estimation of Sensorless Brushless DC Motor Using Sliding Mode Observer

by

Attabik Tabib

(MEE183009)

THESIS EXAMINING COMMITTEE

S. No.	Examiner	Name	Organization
(a)	External Examiner	Dr. Ghulam Mustafa	PIEAS, Islamabad
(b)	Internal Examiner	Dr. Fazal ur Rehman	CUST, Islamabad
(c)	Supervisor	Dr. Aamer Iqbal Bhatti	CUST, Islamabad

Dr. Aamer Iqbal Bhatti
Thesis Supervisor
November, 2022

Dr. Noor Muhammad Khan
Head
Dept. of Electrical Engineering
November, 2022

Dr. Imtiaz Ahmad Taj
Dean
Faculty of Engineering
November, 2022

Author's Declaration

I, **Attabik Tabib** hereby state that my MS thesis titled "**Back-EMF Estimation of Sensorless Brushless DC Motor Using Sliding Mode Observer**" is my own work and has not been submitted previously by me for taking any degree from Capital University of Science and Technology, Islamabad or anywhere else in the country/abroad.

At any time if my statement is found to be incorrect even after my graduation, the University has the right to withdraw my MS Degree.

(Attabik Tabib)

Registration No: MEE183009

Plagiarism Undertaking

I solemnly declare that research work presented in this thesis titled "**Back-EMF Estimation of Sensorless Brushless DC Motor Using Sliding Mode Observer**" is solely my research work with no significant contribution from any other person. Small contribution/help wherever taken has been duly acknowledged and that complete thesis has been written by me.

I understand the zero tolerance policy of the HEC and Capital University of Science and Technology towards plagiarism. Therefore, I as an author of the above titled thesis declare that no portion of my thesis has been plagiarized and any material used as reference is properly referred/cited.

I undertake that if I am found guilty of any formal plagiarism in the above titled thesis even after award of MS Degree, the University reserves the right to withdraw/revoke my MS degree and that HEC and the University have the right to publish my name on the HEC/University website on which names of students are placed who submitted plagiarized work.

(Attabik Tabib)
Registration No: MEE183009

Acknowledgement

First and foremost to the creator, the most gracious, the most beneficent, the Almighty **ALLAH S.W.T**, I owe it all to you, Thank you!

There have been many people who have walked alongside me, who have guided me through all these efforts. I would like to outstretch gratitude to each one of them. Topping the list is my supervisor **Dr. Aamer Iqbal Bhatti** to whom I owe my deepest gratitude for providing his valuable guidance to complete this research. Besides that, I am also very grateful to my teachers for their unconditional help as well as technical & motivational support thorough out the research journey.

Furthermore, I owe a great deal to my parents who shaped me into the person I am today. Their continuous support and encouragement made this work possible.

(Attabik Tabib)

Abstract

The emission of carbon dioxide from combustion engine of vehicles has become an important issue because it is affecting the environment. New engines based on different motors have been developed with reduced carbon dioxide emissions. A Brushless Direct Current (BLDC) motor is selected in our research because it has significant features like good torque/speed characteristics, low noise, high efficiency and so on as compared to other motors used in Electric Vehicles (EVs). With the increasing demand of BLDC motor, its control for different industry requirements has seen some challenges. Different techniques have been implemented to control the BLDC motor. Our focus is on the estimation of the Back Electromotive Force (Back-EMF) of a three-phase sensorless BLDC motor. Back-EMF signal is important because it is used to generate the switching signals that are required to operate a BLDC motor drive. In previous research, different techniques based on linear and non-linear observers were implemented to estimate the back-EMF. One of these techniques is a Sliding Mode Observer (SMO). This technique is selected because of its robust performance. SMO is designed using Signum function. Stator Voltages and currents of the motor are used as inputs in observer design. The implementation of the back-EMF estimation is done using MATLAB/Simulink which is a widely used tool for simulation purposes. There are total six outputs of the observer. Observer estimates three currents and three back-EMFs of the motor. The proposed design is quite simple and effective as compared to previously implemented observers which had complex designs involving multiple signal transformations. This technique has replaced the use of costly hall sensors which are used to get position of the rotor for back-EMF generation. SMO has very good performance in estimating the current and back-EMF. The estimation results are compared with the previous research results to check the performance of SMO and the accuracy of the results.

Contents

List of Figures

List of Tables

Abbreviations

BLDC	Brushless Direct Current
EVs	Electric Vehicles
EMF	Electromotive Force
IM	Induction Motor
PMSM	Permanent Magnet Synchronous Motor
SMO	Sliding Mode Observer
SMC	Sliding Mode Control
ZCD	Zero Crossing Detection
ZCP	Zero Crossing Points

Symbols

L	Stator phase inductance of BLDC motor
M	Mutual inductance between phases of BLDC motor
R	Stator phase resistance of BLDC motor
Δ	Unmodeled dynamics of BLDC motor

Chapter 1

Introduction

1.1 Background

Scholars have presented a basic definition of a **Brushless Direct current(BLDC) motor**. Some researchers presented that only the trapezoidal/square wave motors can be called BLDC Motors, while sinusoidal wave motors should be termed as Permanent Magnet Synchronous Motors(PMSM). The definition in NEMA Standard MG7-1987 describes the BLDC motor as a self-synchronous motor where the rotor is a permanent magnet and the electronic commutation process controls the motor. This commutation hardware can be integrated with the motor or can be independent. Moreover, there are sensors for rotor position sensing. This book [1] considers the BLDC motor as a trapezoidal/Square wave motor with the characteristics of series and shunt excitation DC motors. It has advantages like large torque, high efficiency and simple structure. A motor has different applications in all kinds of fields. With respect to their applications, different motors like an induction motor, synchronous motor, DC motor, switched reluctance motor and so on have been developed over the years.

Synchronous motor has a lot of advantages like high efficiency, high torque and good mechanical characteristics but it has disadvantages in regulation of speed. An induction motor has the advantages of low price, simple structure and easy

fabrication but it has issues of power factor, start up mechanical characteristics and uneconomical speed regulation of wide speed range. A switched reluctance motor has a simple structure if its rotor does not have windings or permanent magnet on its rotor. At low speed, high torque can be produced by a switched reluctance motor, but it has disadvantages like torque ripples and the noise generated. DC motor has advantages of good speed regulation and high performance, therefore it has demand in electric traction. In DC motors, the commutation is done by brushes, which result in electric spark, noise and mechanical friction. The disadvantages like the maintenance and high cost of production limit the applications of DC motors in different areas. Therefore, the requirements of motor with high performance has increased [1].

1.1.1 History of BLDC Motors

To counter the issues of brushed DC motors, BLDC motors were developed. The electromagnetism induction phenomenon was established by Faraday in 1831. BLDC motor could not be developed at that time because there were no adequate magnet materials and power electronics devices to run the motor. In 1915, DC/AC converter was made by Langmuir. After the development of this converter, the research was started on BLDC drive system. BLDC motor development was started with electronic commutation. However, this motor had low efficiency and less reliable for work due to the fact that the commutation device and other power electronics devices at that time were in early stages of development. In 1955, the first thyristor based commutation circuit patent claim was made by Harrison and Rye. Traditional mechanical commutation equipment was replaced by this electronic commutation circuit. The operating principle of this motor is that Electromotive force (EMF) is induced in the winding when the rotor is rotating. This EMF is then used for the conduction of thyristors. All the windings feed by turns result in the commutation. However, there were some problems. The EMF is not produced in the winding when the rotor is not rotating. As a result, thyristor is not biased and the current cannot be fed by the power winding. Due to these

problems, there is no starting torque of BLDC motor. To resolve these issues, researchers introduced the following solutions:

1. A Commutator with Centrifugal Plant was introduced.
2. To ensure the reliable start of the motor, an accessory steel magnet was used.

Multiple practices and experiments were performed to overcome the issues of BLDC motor. As a result, in 1962, a BLDC motor with electronic commutation using hall elements was developed. A diode with magnet sensing capability was used to control the BLDC motor in 1970s. This diode had sensitivity thousands of times greater than that of hall elements used at that time [1].

1.2 Construction and Working Principle of Brushless DC Motor

Brushless DC motor is related to synchronous motor because the frequency of the magnetic field of rotor and the magnetic field produced by stator have the same frequency. This motor also has the advantage that it does not experience the **slip** as experienced by induction motor. BLDC has following three basic configurations:

1. Single-Phase Motors
2. Two-Phase Motors
3. Three-Phase Motors

Three-phase BLDC motors are mostly used as compared to other mentioned configurations. We will focus on the construction of a three-phase BLDC motor as compared to other above mentioned configurations. A brushless DC motor has a similar construction as of a permanent magnet synchronous motor (PMSM). Let

us discuss the construction of this motor in detail. Commutation is done using mechanical brushes in traditional DC motors. These mechanical commutators were replaced by an electrical switch circuit in the BLDC motor drive system. In addition, rotor position sensor and three-phase inverter are required in order to control the BLDC motor position and speed. Let us discuss the structure of the rotor and stator of a BLDC motor.

1.2.1 Stator of a Brushless DC Motor

A Brushless DC motor has a rotor made up of a permanent magnet while the stator is constructed using windings. This structural design is similar to that of a permanent magnet synchronous motor (PMSM). The stator has windings arranged in slots and stacked steel laminations. This stator is similar to that of an induction motor, but the distribution of windings is different. The stator of a Brushless DC motor can be seen in Fig. 1.1.

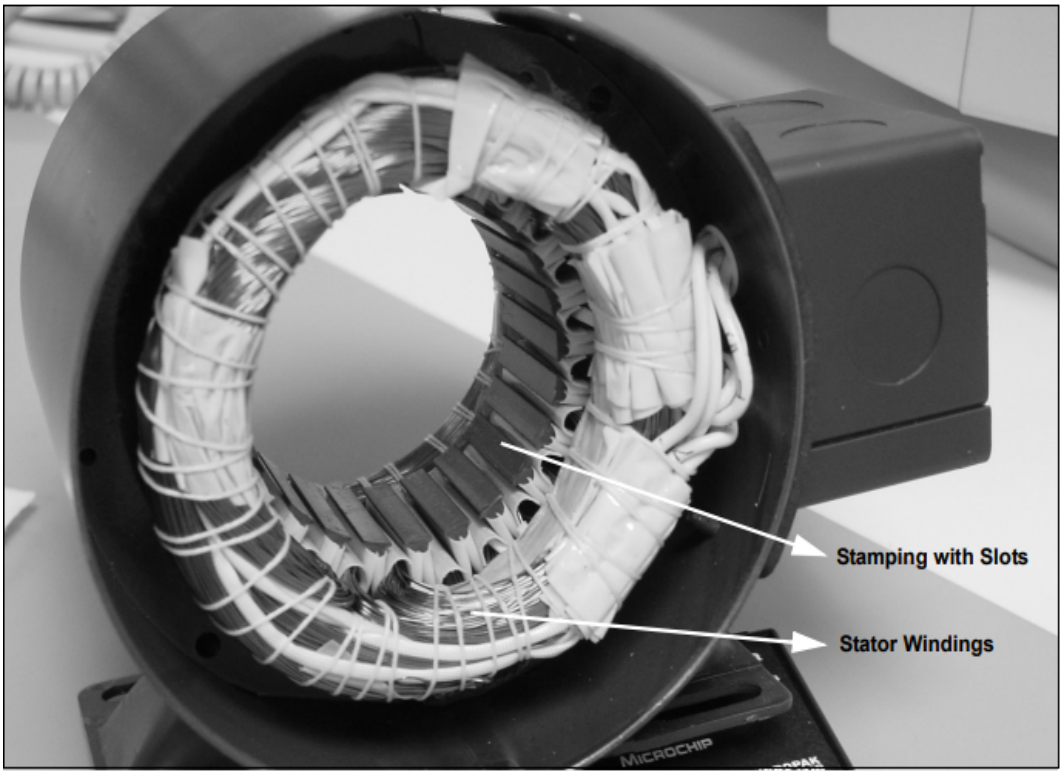

FIGURE 1.1: Stator of a Brushless DC motor [2]

Generally, the motor has three windings connected together in start configuration. Each winging is constructed using interconnection of numerous coils. The slots have one or more coils interconnected to form a winding. All these windings are arranged in the stator in such a way that results in even number of poles. Following are the two variants of stator windings:

1. Trapezoidal
2. Sinusoidal

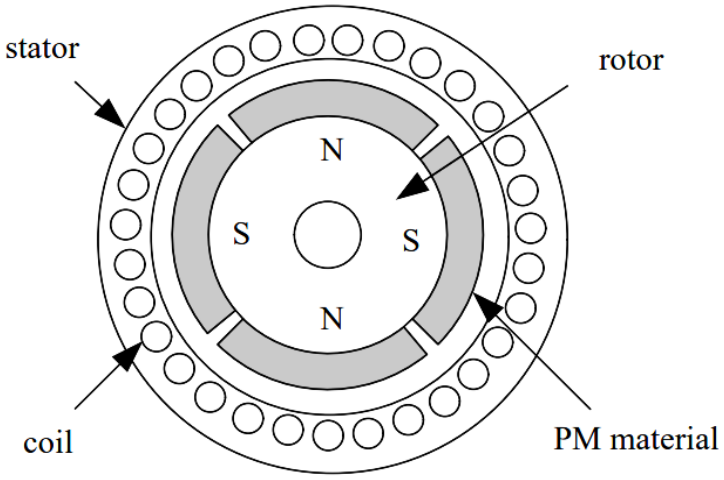

FIGURE 1.2: Stator of a Four Pole BLDC motor [1]

A cross-sectional view of the stator of a Brushless DC motor can be seen in Fig. 1.2. This difference in the trapezoidal and sinusoidal back-EMF is produced due to the coils connection in the windings of stator which result in different back-EMF [2]. A question here arises that what is back-EMF. Let us discuss this concept.

1.2.1.1 Back Electromotive Force (EMF)

A force is generated in each winding when the BLDC motor rotates. This force is known as **Back Electromotive Force** or **Back-EMF**. The principle of the Lenz's Law states that this force opposes the main voltage supplied to the winding. The force has an opposite polarity as compared to the main energized voltage. Back-EMF relationship can be given as:

$$\text{Back EMF} \propto \text{N}lr\text{B}\omega \tag{1.1}$$

Where:

The number of winding turns per phase is represented by N

Rotor length is represented by l

Rotor internal radius is represented by r

Magnetic field density of rotor is represented by B

Angular velocity of motor is represented by ω

The number of turns in windings of stator of the BLDC motor and the magnetic field of rotor cannot be changed once the motor is designed. The only variable that can affect back-EMF signal is the rotor speed. It can be seen that there is a direct relationship between rotor speed and back-EMF. The shape of EMF of trapezoidal motor is trapezoidal as shown in Fig. 1.3.

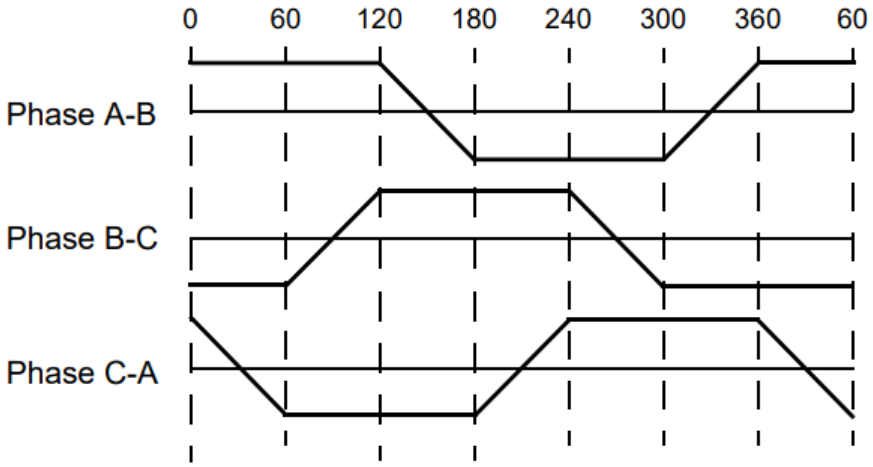

FIGURE 1.3: Back-EMF with Trapezoidal Shape [2]

The shape of back-EMF of sinusoidal trapezoidal motor is sinusoidal as shown in Fig. 1.4. Motors with rated voltage of $48V$ or less are used in robotics, small arm movements automotive and so on. Motors with rated voltage of $100V$ or above are used in automation, appliances and industrial applications.

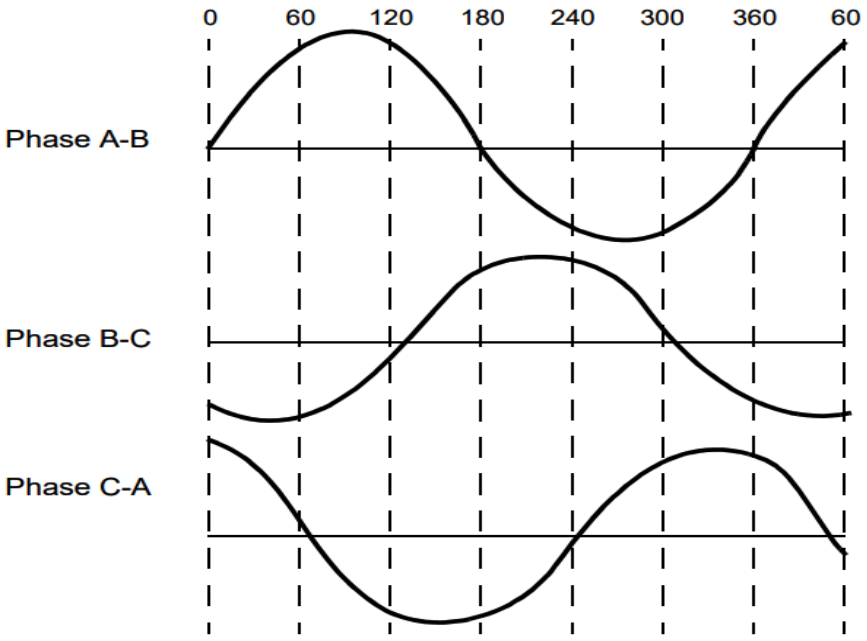

FIGURE 1.4: Back-EMF with Sinusoidal Shape [2]

1.2.2 Rotor of a BLDC Motor

Permanent magnets are used to make the rotor of a BLDC motor. A BLDC motor has at least two poles and the poles can extend to eight. Fig. 1.5 shows the cross section of a rotor magnet with different arrangement of magnets.

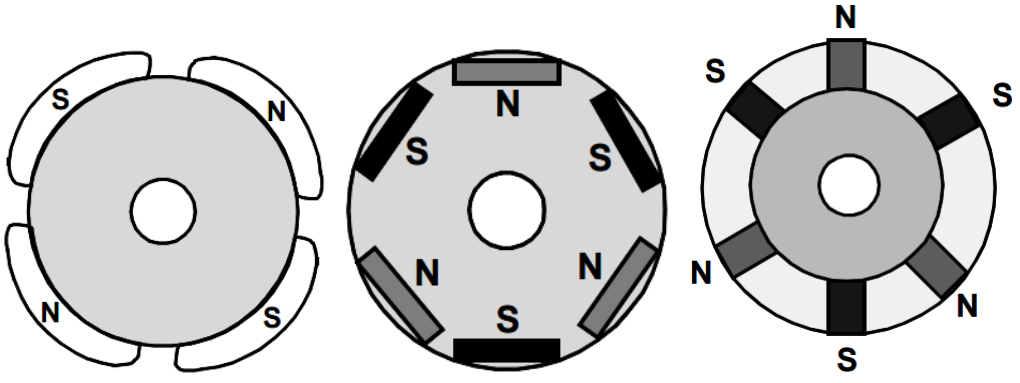

FIGURE 1.5: (a) Rotor with Circular Core and Magnets on the Periphery (b) Rotor with Circular Core and Embedded Magnets (c) Rotor with Circular Core and Rectangular Magnets Inserted into Rotor Core [2]

According to the requirements of rotor magnetic field density, the material of the magnet is selected. Generally, Ferrite magnets are used to make a permanent magnet. Ferrite magnets are cheap, however, they have some disadvantages like

low flux density for a given volume. In comparison, alloy material has a high flux density for a given volume. Therefore, alloy materials have advantages in terms of size-to-weight ratio. Alloy materials also give high torque with small motor size as compared to ferrite magnets with the same size.

1.2.3 Hall Sensors

BLDC motor commutation is done electronically as compared to a brushed DC motor. The stator windings must have a proper energizing sequence, so that the motor could run smoothly. For this purpose, the rotor position can help us in determining the sequence to energize the respective winding. Hall effect sensors are used to sense and provide the information about the rotor position. In most BLDC motors, the stator has three hall sensors embedded in it as shown in Fig. 1.6.

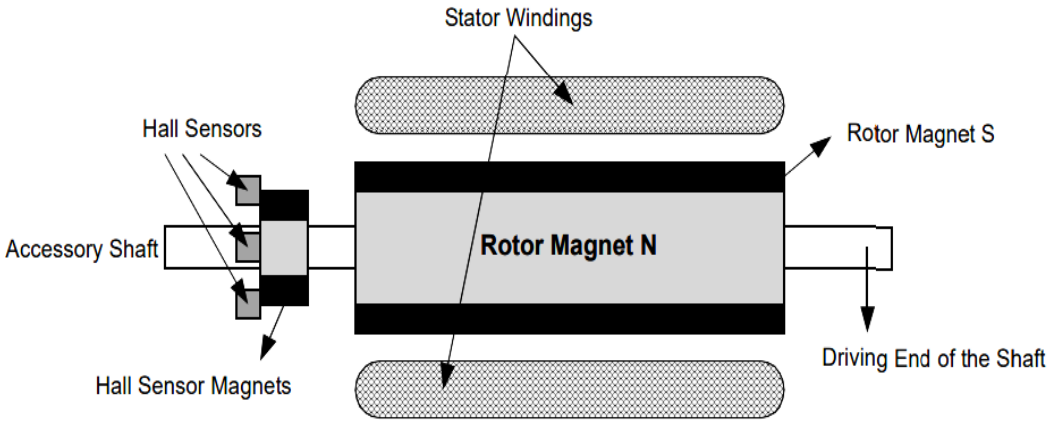

FIGURE 1.6: BLDC Motor Transverse Section [2]

These sensors work on the basis of **Hall Effect** theory that was discovered by E. H Hall in 1879. The hall sensors produce a HIGH or LOW output signal when the rotor magnetic poles pass near to them. This combination of three outputs from three hall sensor give a sequence which is used for commutation of the motor.

1.3 Motors used in Electric Vehicles

The history of the most commonly used motors for commercial electric vehicles is presented in [3]. According to this research, there are four types of motors used in electric vehicles. Following are the motors discussed in this research:

1. Permanent Magnet Synchronous Motor (PMSM)
2. Brushless Direct Current (BLDC) Motor
3. Induction Motor (IM)
4. Switched Reluctance Motor (SWR)

Another research on commonly used motors for electric vehicles is presented in [4]. The classifications of these motors can be seen in Fig. 1.7.

1.3.1 Comparison of a Brushless DC Motor with Other Motors

A BLDC can be compared with an induction motor on the basis of multiple factors that should be considered while selecting a BLDC motor [2]. This motor has the following features that make it favorable as compared to an induction motor:

1. Good characteristics of speed and torque.
2. Output power to size ratio: High output power can be achieved with small motor size.
3. Extra starter circuit is not required.
4. No slip.

In comparison with a brushed DC motor, a brushless DC motor has an upper edge on the basis of the following features:

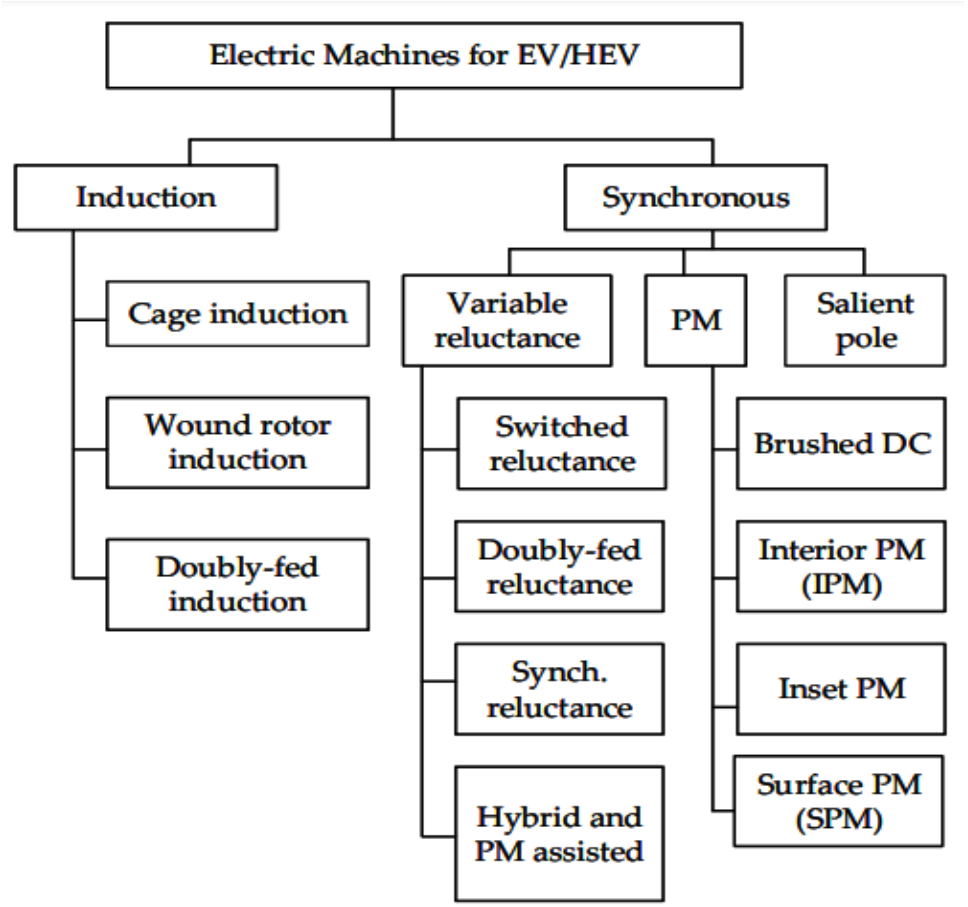

FIGURE 1.7: Motors for EV and HEV

1. Low maintenance requirement because there are no brushes.

2. Good characteristic of speed and torque.

3. High output power to size ratio: High output power can be achieved with small motor size.

4. Electronic commutation on the basis of Hall sensors.

5. Good range of speed.

6. Low noise.

7. High efficiency.

8. Reliable and has longer life.

1.3.2 Significance of BLDC Motor in Different Industries

BLDC motor is preferred over other motors due to its performance in different industries like automotive industry, pumping industry, etc. [5].

Although BLDC motor has been accepted as an efficient and reliable motor to drive electric vehicles but its main purpose is to control the emission of carbon dioxide from traditional combustion engines is a highlighted regarding environmental sustainability. The development of engines of electric vehicles had a great affect on emission levels [6].

We are using BLDC motor in our research. Our main focus is on the estimation of back-EMF for sensorless motor. The literature survey of related techniques and details of the proposed technique along with our objectives are discussed in Chapter 2.

1.4 Applications of BLDC Motors

There are numerous applications of BLDC motor in different industries like automotive industry, aviation industry, appliances etc. These applications depend upon different load requirements [2]. Table 1.1 represents the BLDC motor applications which have constant load conditions. Examples like fans and blowers are mentioned because they require variable speed control during their operation.

Table 1.1: Constant Load Requirements

SN	Application
1	Pumps
2	Fans
3	Blowers

Table 1.2 represents the applications of BLDC motors. These applications are specific to variable load requirements. Here, we can see that electric vehicles are also mentioned. Our research is related to those electric vehicles which have BLDC motors.

TABLE 1.2: Varying Load Requirements

SN	Application
1	Compressors
2	Home Appliances
3	Dryers
4	Washers
5	Robotic Arm
6	Electric Vehicles

1.5 Summary

Carbon dioxide emission from traditional combustion engines of cars has severe effects on the global environment. Researchers have proposed new all-electric engines for cars known as Electric Vehicles (EVs). Due to this concept of electronic commutations, the BLDC motor has gained popularity in the automobile industry. BLDC motor is also preferred over other motors due to its performance in different industries like automotive industry, pumping industry and so on. The history, construction, working principle and applications of this motor are discussed in this Chapter. Also, the features of this motor are discussed which make it suitable for different applications. The details of different techniques to implement our research are discussed in Chapter 2.

Chapter 2

Literature Review

2.1 Introduction

The importance and use of BLDC motors in industries are increasing due to their numerous applications such as in the automotive industry. Due to this fact, the challenges regarding the performance, durability and reliability of the motor are also faced by the researchers [5]. There are two different controls of the BLDC motor. The first one is sensorless control and the other is with sensors. Position sensors known as Hall sensors are used in sensor-based control. Our research is focused on sensorless control of BLDC motor.

2.2 BLDC Motor Control Methods

There are two main methods of BLDC Motor Control:

1. Hall Sensor Based Control Method
2. Sensorless Control Method

Hall sensors are used to get the position of the rotor which is then used to generate back-EMF and commutation signals in order to operate and control the BLDC

motor. Sensorless techniques do not use hall sensors for rotor position detection. In sensorless methods, different waveforms like rotor position and back-EMF waveform are determined or estimated using different techniques and then used to generate commutation signals for switches in order to operate and control the BLDC motor. As already mentioned initially, our main focus in this research is on the back-EMF estimation of sensorless BLDC motor. Therefore, we have focused only on the methods used for back-EMF estimation of a sensorless motor control system.

2.2.1 Sensorless Control of BLDC Motor

Sensorless control of a BLDC motor can be implemented with the help of different techniques. The details of these techniques mentioned in the literature are discussed in this chapter. One of the commonly used techniques is back-EMF based control. In this technique, the back-EMF profile of the motor is determined or can be estimated in order to operate and control the BLDC motor. Following are some of the control techniques which depend on excitation signal.

1. Open-Loop Techniques
2. Closed-Loop Techniques
3. Observer-Based Techniques

The selection of the control method depends upon the characteristics and the type of the motor [7]. Some other sensorless control techniques that are implemented previously as mentioned in [8] are:

1. Phase Current Sensing Method
2. Back-EMF Zero Crossing Point Detection
3. Detecting Third Harmonic of Back-EMF
4. Back-EMF Integration Method

2.2.1.1 Back-EMF based Position Detection Techniques

To control a BLDC motor, the position of rotor is required. Sensorless motor control is better in term of cost and reliability as compared to other available position sensor based products. Rotor position can be determined using different methods for sensorless motor control.

One of the methods is to determine rotor position using Back-EMF. When the rotor of permanent magnet motor moves, the Back-EMF signal is generated and the position of rotor is directly proportional to its speed. The shape of the EMF is trapezoidal. There are different methods for detection of back-EMF. Most methods use motor voltages with respect to motor neutral point for detection. These detection methods have disadvantages at low speed. One technique that is used for motor control is to detect and use the third back-EMF harmonic for rotor position detection. Even at low speed, the third harmonic can be detected [7].

2.2.1.2 Zero Crossing Detection Technique

A common technique used for sensorless control is Zero Crossing Detection (ZCD) as mentioned above. At first, line voltages are sensed. Line-to-line voltages are generated using the information of line voltages. The difference between the line-to-line voltages is determined as shown in Fig. 2.1.

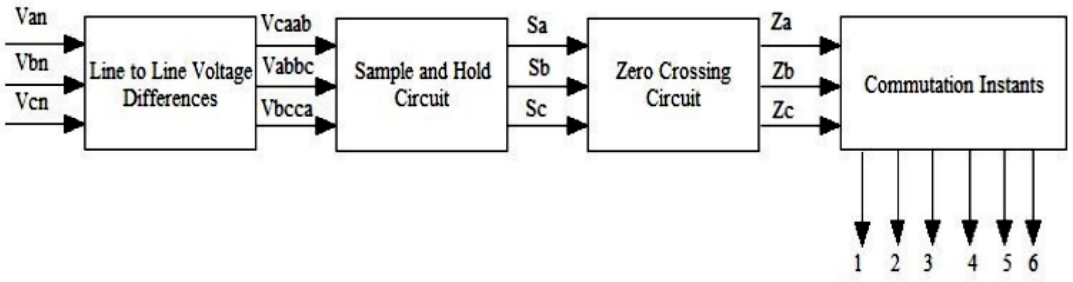

FIGURE 2.1: Implementation Procedure of Zero Crossing Detection [9]

Zero crossing points are determined using these difference voltages. Commutation sequence for the inverter switching is generated using the zero cross points and fed to the decoding system to control the motor [9]. Because of the direct relationship

between Back-EMF and rotor speed, the ZCD detection method provides good performance at high speed [10].

2.2.1.3 Linear Observer for Back-EMF Estimation

Observer-based techniques involve back-EMF estimation using different input signals like motor voltages and currents. Different methods are used for sensorless control but they do not have good performance at low speed. An observer-based technique in [8] has implemented an observer with unknown input as shown in Fig. 2.2.

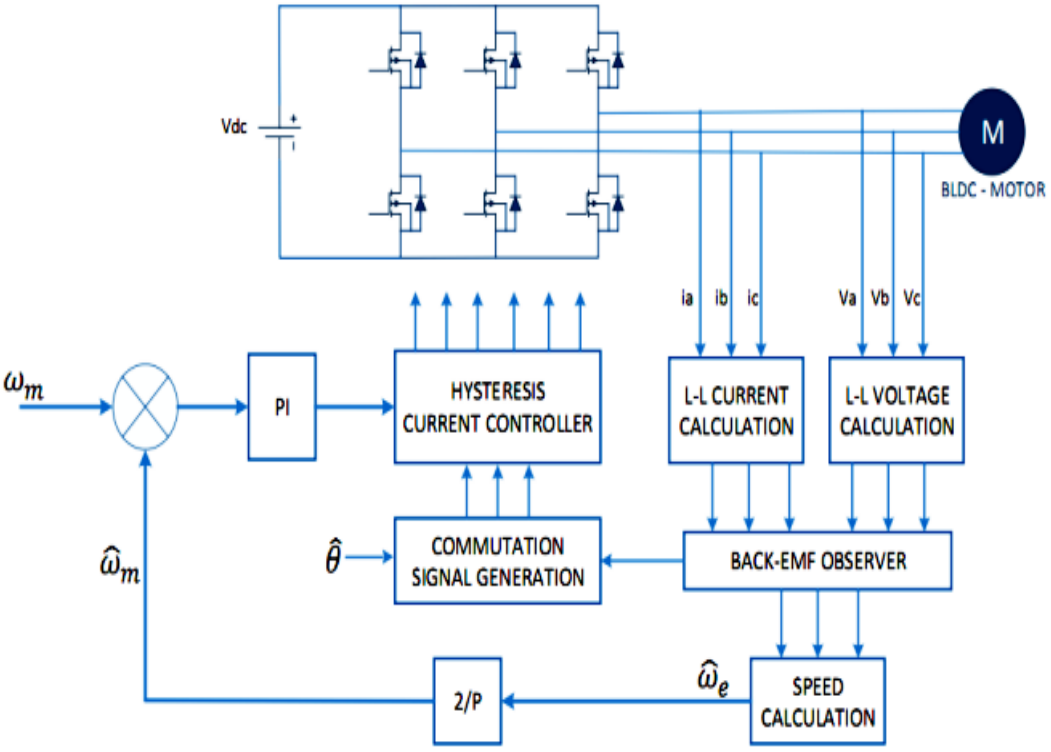

FIGURE 2.2: An Unknown Input Observer based Sensorless BLDC Motor Control System [8]

The unknown input is back-EMF signal which is modeled and has a trapezoidal nature. Rather than calculating the back-EMF of each phase, the difference of back-EMF between two phases is estimated using the proposed scheme which is then used to determine the rotor position and eventually getting a good performance for low-speed also. A different observer based technique is also implemented

in previous research as shown in Fig. 2.3. DC bus voltage is used to determine the line to line voltage which is then used in the observer. The dependency of the neutral voltage is eliminated using this technique and zero crossing detection is not required. The difference of back-EMF along-with back-EMF signal is estimated. Also, the speed and position of BLDC is properly estimated using this observer [11].

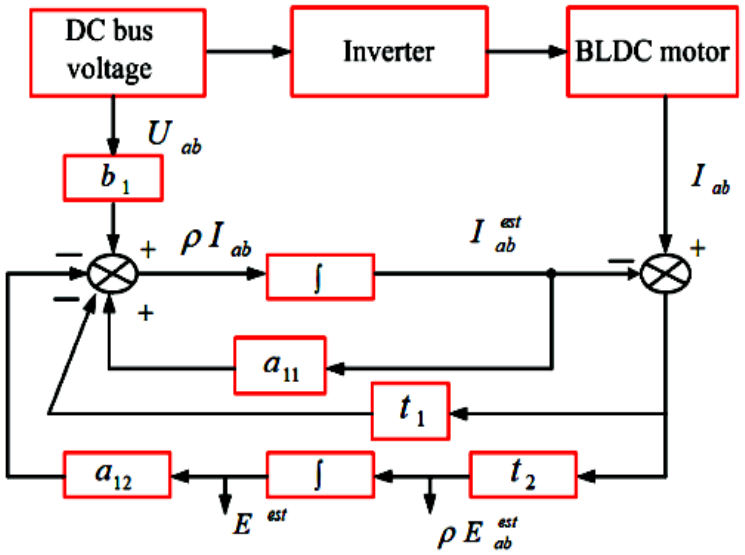

FIGURE 2.3: Observer Configuration [11]

The above discussed observer has the following limitations:

1. At low reference speed, the estimated speed and back-EMF results show oscillations when load torque is changed. this behaviour is not suitable for a motor operation.

2. The comparison of back-EMF of all phases is not presented, so, we cannot verify the accuracy of estimated EMF in terms of phase shift and shape/-pattern.

Another implementation of a robust and simple Back- EMF observer can be seen in Fig. 2.4. The observer estimates the line to line back-EMFs which do not depend on the rotor speed. Due to this fact, the this technique gives good performance at high speed as well as at low speed [10].

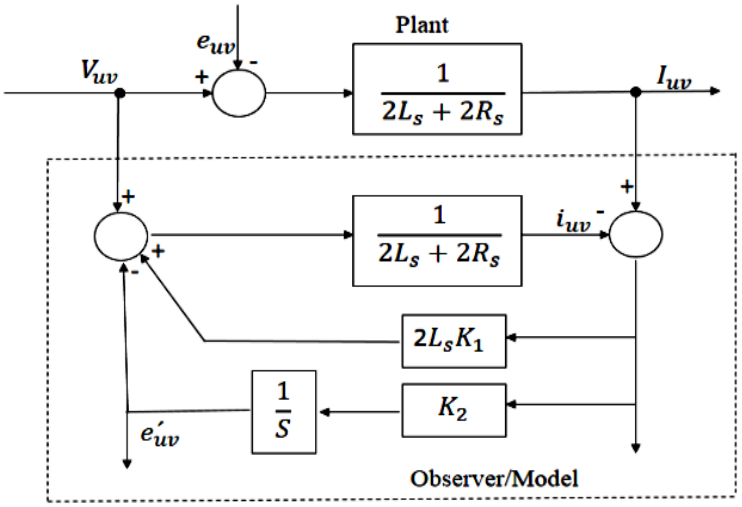

FIGURE 2.4: Observer Block Diagram [10]

2.2.1.4 Sliding Mode Observer for Back-EMF Estimation

In previous research, different implementations of back-EMF estimation for sensorless BLDC motor is done. One of these implementation can be seen in this research [12].

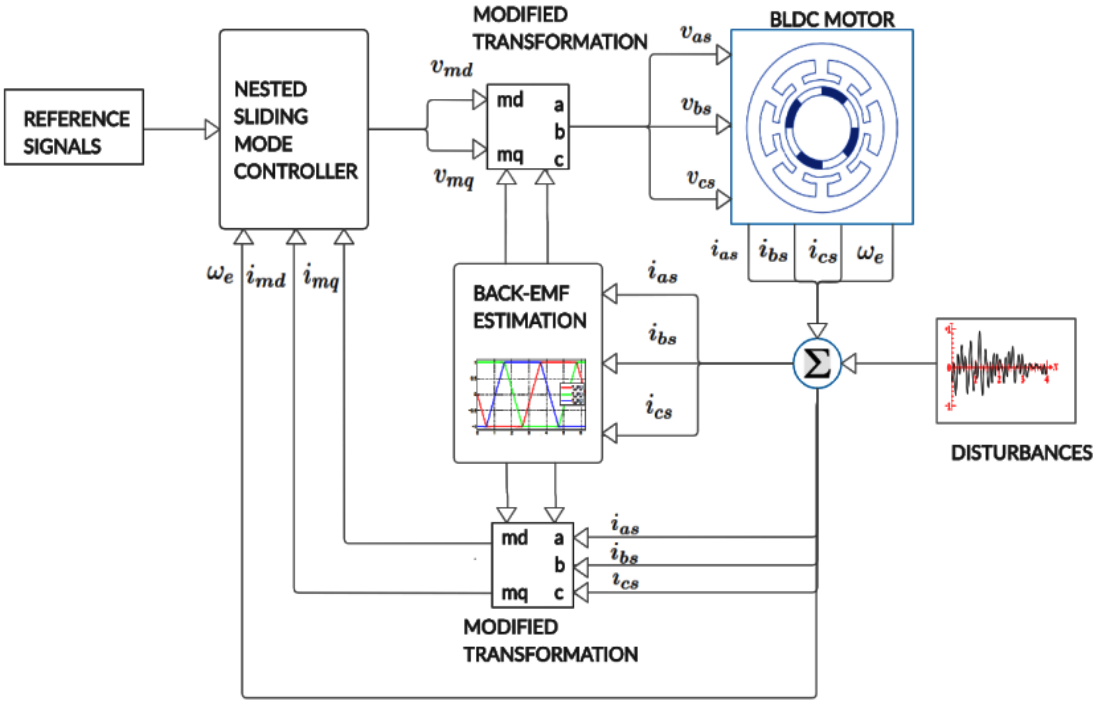

FIGURE 2.5: Block Diagram [12]

A second order sliding mode observer is used for estimating back-EMF as shown in Fig. 2.5. A closed loop systems with Park transformation for signals is used to implement field oriented control of the BLDC motor on the basis of back-EMF estimation. The design also includes a nested sliding mode control scheme in order to cater the unmatched disturbance signals as well.

The above mentioned BLDC motor control system has following limitations:

1. Proposed SMO model needs rotors position for estimation. Rotor position is not directly accessible in sensorless BLDC motors.

2. Additional signal transformations (i.e. Clarke and Park Transformations) to implement the observer which makes the design more complex.

Another SMO has been implemented in previous research for estimation of back-EMF, speed and position of the rotor as shown in Fig. 2.6. The observer is used in the implementation of a sensorless BLDC motor control system [13].

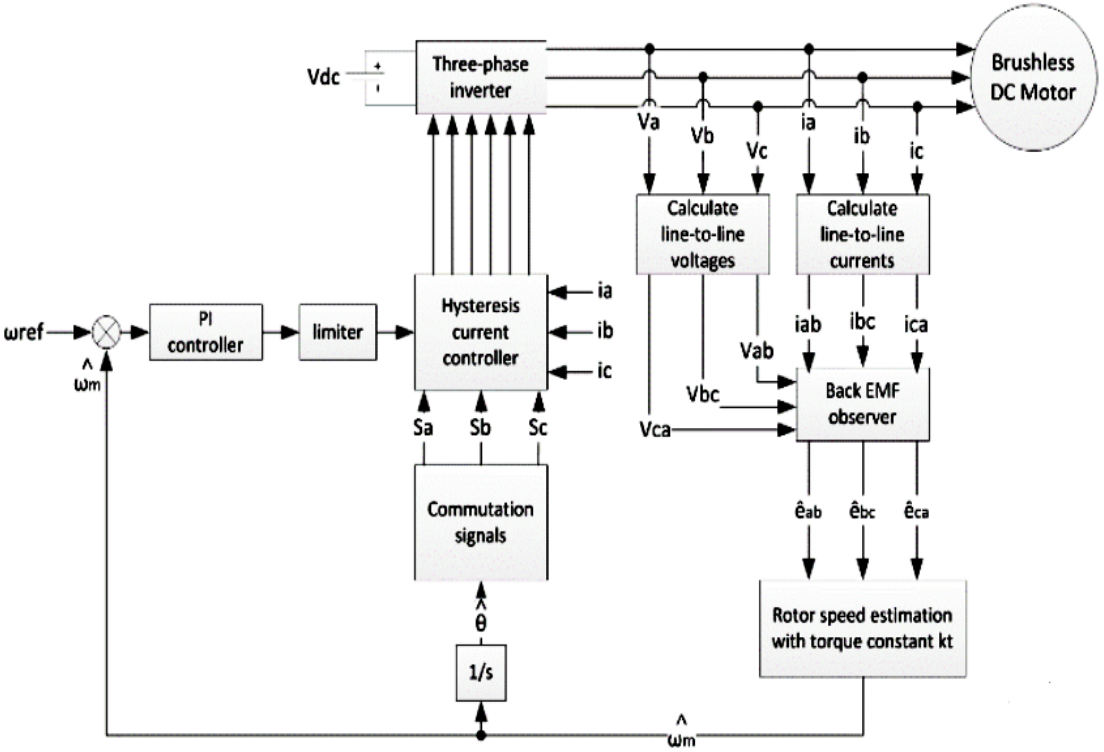

FIGURE 2.6: BLDC Motor Drive [13]

The system calculates line-to-line voltages and line-to-line currents from measured values of line voltages and line currents. A sliding mode observer is used that estimates line-to-line back-EMF signals of all phases during first stage. In the second stage, the estimated back-EMF signals are used for estimating the speed and position of the rotor. Results of stator current (i_a), Rotor speed, Back-EMF (e_a) and Electromagnetic Torque are compared with the results of control methods like direct back-EMF control using ZCP detection and Hall Sensor based control. The results of Hall sensor based method and the proposed method of this paper have good results as compared to direct back-EMF control method. The proposed method provides a good control of speed and detection of rotor position over wide range of speed. There are following disadvantages of above discussed SMO:

1. Back-EMF is taken as an unknown state but the model dynamics of this states are not defined.
2. The estimated state result has a lot of chattering.
3. The estimated results are not suitable and cannot be used for control purpose of BLDC motor.

Field Oriented Control (FOC) of a BLDC motor with the help of a Sliding Mode Observer (SMO) is presented in another research [14]. In this case, a set of observers is used. The first observer (current observer) has been used for estimating the currents while a second observer (back-EMF observer) has been used for estimating the rotor speed and position of the motor. In order to reduce the chattering effect, the Saturation function is used instead of the Signum function. A comparison with the conventional SMO is also presented [14]. The estimation results show that this proposed SMO has better performance as compared to conventional SMO.

The above discussed implementation has the following disadvantages:

1. A complex set of observers was designed which is hard to implement in real time regarding processing power requirements.

2. EMF results are not shown, so, we cannot verify the performance of the second observer which is used for back-EMF estimation.

2.3 Highlighted Issues of Brushless DC Motor

BLDC Motor control has its own issues and disadvantages. Some important issues are discussed in this section.

2.3.1 Cost and Maintenance Issue

The signals generated by hall sensors are used to drive BLDC motor. Due to vibrations and other issues, the hall sensors are prone to damage which makes the motor less reliable for use in harsh environments. The maintenance of damaged hall sensors is not easy because they are mounted on the stator inside the motor. On the other hand, the use of hall sensors results in increasing cost of motor. Therefore, the sensorless control methods are becoming an important research topic. Another issue is non-ideal waveform of back-EMF. Most of the previous research methods assume that the back-EMF waveform is trapezoidal. Actually, the waveform is not completely trapezoidal due to manufacturing and design defects in BLDC motors [11], [15].

2.3.2 Motor Size and Control Unit Cost Issue

Hall sensors are mostly used to get the information about rotor position. Additional hardware control unit is required to process this information. This results in increased cost due to additional hardware control unit and wired connections for hardware applications. The overall size of the motor and controller cost increases due to the use of sensors [8].

2.3.3 Limitations of Zero Crossing Detection Technique

Zero Crossing Detection (ZCD) technique has a good performance at high speed. But, at low speed, there is no adequate information of back-EMF which results in poor performance of motor at low speed [10].

The output information of the ZCD technique will not be accurate if the ZCD technique has limitations and not implemented accurately [11].

It is very difficult to detect the zero crossing points of back-EMF at very low speed or standstill conditions. An adequate acceleration of the motor is required in order to detect the back-EMF. Commutation instants depend upon the line voltages. Line voltages need to be measured and filtered to enhance the quality and to shift the phase for further use [13].

2.3.4 Limitations of Back-EMF Integration Technique

A back-EMF integration technique has been implemented in previous research which gives rotor position information using ZCD. The disadvantage of this technique is that it does not give proper information about the rotor position. Also, there is no synchronization between back-EMF and stator current [10].

The noise generated as a result of switching has less effect on this technique. However, at low speed, it has poor performance [11].

2.4 Gap Analysis

Different techniques of back-EMF estimation of sensorless BLDC motors are discussed in this Chapter. Some of these techniques are based on linear observers while some are based on SMO. Sliding mode observer is a non-linear observer and is preferred for its robust performance. Techniques that have been previously implemented had good performance based on their proposed design but they also

had some limitations or disadvantages as discussed in the literature review. Based on this literature survey, The following analysis was made:

1. Overall complexity of observer design needs to be reduced. The use of complex transformations makes the observer design complex. A simple observer is required for back-EMF estimation in order to implement it in real-time applications.

2. Limitations in observer algorithm design and implementation resulting in improper results should be addressed and resolved.

3. Generally, back-EMF generation/estimation is not accurate at low speed as observed in the zero crossing detection technique. This issue should be resolved.

The summary of the techniques used and limitations in the previous research are presented in Table 2.1.

TABLE 2.1: Gap Analysis

Reference	**Authors, Year**	**Estimation Technique**	**Limitations**
[11]	Shrutika *et al*, 2021	Linear Observer	Oscillations are generated in the back-EMF results at low reference speed when the load torque is changed. The comparison of back-EMF of all three phases is not presented, so, we cannot verify the accuracy of the estimated back-EMF in terms of phase shift and shape/pattern.

[12]	Alanis *et al*, 2020	SMO	SMO requires rotor position for the estimation which is not directly accessible in sensorless BLDC motors. Signal transformations (i.e. Clarke and Park Transformations) are used to design the observer making the design complex.
[13]	Topal *et al*, 2019	SMO	This paper is considering the back-EMF as an unknown state without having valid model dynamics. The estimated state result has a lot of chattering. The estimation results are not suitable and cannot be used for control purposes of the BLDC motor.
[14]	Hernandez *et al*, 2019	SMO	A complex set of observers was designed which is difficult to implement in real-time regarding signal processing requirements. Estimated back-EMF results are not shown, so, we cannot verify the performance of the observer.

2.5 Problem Statement

Due to the limitations of hall sensors, the sensorless motor is selected. These limitations are discussed in **highlighted issues of BLDC motor** section. Different techniques used for estimating back-EMF of Sensorless BLDC motor are presented in this chapter. Because of its robust performance, sliding mode observer (SMO) is selected for estimation of back-EMF. Different implementations of SMO in previous researches are studied discussed along with their limitations. Most of the previous research regarding observers that is discussed in this chapter is focused on Field Oriented Control (FOC) or related techniques in which transformations are required from one reference frame to another e.g Clarke Transformation and Park Transformation. The use of these transformation add complexity to the design of the observer because the signals need to be transformed during intermediate stages and then transformed back to the original reference frame before getting the final output.

Another issue as seen in [12] is that the researchers have used the function of rotor position in the design of observer. For sensorless motor, the rotor position is not available or cannot be accessed directly from the motor. This adds uncertainty in the design of the observer. Although the SMO is thought to have good performance and robustness, but in some cases as seen in [13], the estimated results show significant chattering. These results cannot be used to drive a BLDC motor specially in hardware implementation. Such observer designs have not shown good performance due to limitations in their design.

Our goal is to propose a simple and effective SMO that is able to solve the issues discussed above. The design of the observer is given in the next chapter.

2.6 Summary

Speed control of BLDC motors is becoming an important research topic because of the environmental effects caused by standard combustion engine based motor drive

systems. To get a sustainable solution for motor drive systems, BLDC motors are preferred because of their fully electronic control system. BLDC motors can be controlled with two basic methods. These methods are hall sensor based control and sensorless control. There are various limitations of hall sensor based control which are discussed in this chapter. Due to these limitations, sensorless control is preferred. There are various techniques to implement the sensorless control which are discussed and evaluated in this Chapter. One such sensorless technique is to control the BLDC motor using back-EMF signals. Our focus is not on the control of the motor rather our main objective of this research is to estimate the back-EMF signals that can be used to drive the motor. Various estimation methods/techniques are discussed and evaluated. The sliding mode observer (SMO) technique is selected after thorough research and the research gap is also analyzed. The design details of SMO and BLDC motor are given in Chapter 3.

Chapter 3

Modeling of a BLDC Motor and Observer Design

3.1 Introduction

3.2 BLDC Motor Model

An equivalent circuit of a BLDC motor is shown in Fig. 3.1 which serves as a model of the BLDC motor.

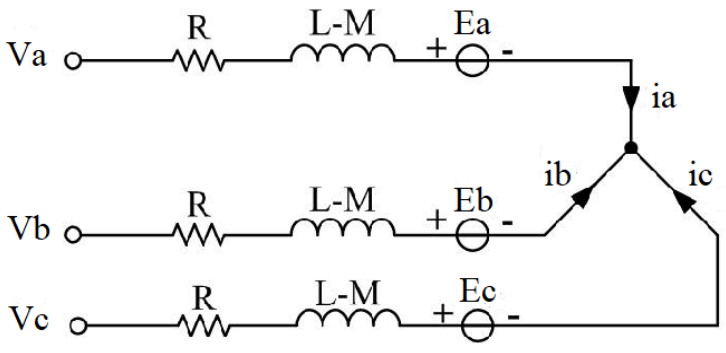

FIGURE 3.1: Equivalent Circuit of BLDC Motor [11]

Here, V_a is Phase-A Voltage

Similarly, V_b is Phase-B Voltage, V_c is Phase-C Voltage

R represents the Stator Resistance of Each Phase

L represents the Stator Inductance of Each Phase

M represents the Mutual Inductance

Δ represents the unmodeled dynamics of BLDC Motor

$E_a, E_b and E_c$ are the Back-Electromotive Forces of Respective Phases

$$V_a = Ri_a + L\frac{di_a}{dt} + M\frac{di_b}{dt} + M\frac{di_c}{dt} + E_a + \Delta \tag{3.1}$$

Eq. 3.1 represents the line or phase-voltage equation of a BLDC motor. The phase voltage depends upon stator current, stator inductance, mutual inductance and back-EMF of respective phase. A unknown term (Δ) is also added in the expression which represents the unmodeled dynamics of the motor. The BLDC motor model that we have used has equation consisting of line-to-line parameters. We are using the model in which line current or line voltages are used as modeled in this paper [5]. As both systems (consisting of line-to-line vs. line parameters based system) cannot be same. So, to convert the system from line-to-line to line parameters, model should be changed accordingly. Therefore, we have added Δ as unmodeled term which represents the unknown parameters that re required as a result of this modeling approach.

$$V_b = Ri_b + L\frac{di_b}{dt} + M\frac{di_a}{dt} + M\frac{di_c}{dt} + E_b + \Delta \tag{3.2}$$

Eq. 3.2 represents the line or phase-voltage equation of phase-B.

$$V_c = Ri_c + L\frac{di_c}{dt} + M\frac{di_a}{dt} + M\frac{di_b}{dt} + E_c + \Delta \tag{3.3}$$

Similarly, Eq. 3.3 represents the line or phase-voltage of phase-C. Let us simplify the three voltage equations of the motor in order to design the sliding mode observer.

$$\begin{bmatrix} V_a \\ V_b \\ V_c \end{bmatrix} = \begin{bmatrix} R & 0 & 0 \\ 0 & R & 0 \\ 0 & 0 & R \end{bmatrix} \begin{bmatrix} i_a \\ i_b \\ i_c \end{bmatrix} + \begin{bmatrix} L & M & M \\ M & L & M \\ M & M & L \end{bmatrix} \frac{d}{dt} \begin{bmatrix} i_a \\ i_b \\ i_c \end{bmatrix} + \begin{bmatrix} E_a + \Delta \\ E_b + \Delta \\ E_c + \Delta \end{bmatrix} \tag{3.4}$$

The system mentioned in Eq. 3.4 represents the set of voltage equations of BLDC motor. A same representation of such system regarding BLDC motor modeling is mentioned and used in [5], [10].

As the BLDC motor is connected in Y configuration, so, it is assumed that the stator currents are balanced.i.e.

$$i_a = i_b = i_c = 0$$

Above expression can be modified in order to write one current term as a combination of other two current terms. This will help us in simplifying BLDC motor equations. We can write i_c as a combination of i_a and i_b as mentioned in Eq. 3.5.

$$i_a + i_b = -i_c \tag{3.5}$$

We can also represent i_a as a combination of i_b and i_c that is given as Eq. 3.6.

$$i_b + i_c = -i_a \tag{3.6}$$

Similarly, we can represent i_b as a combination of i_a and i_c as given by Eq. 3.7.

$$i_c + i_a = -i_b \tag{3.7}$$

We can use Eq. 3.5 for simplifying Eq. 3.1 as given below:

$$V_a = Ri_a + L\frac{di_a}{dt} + M\frac{d(i_b + i_c)}{dt} + E_a + \Delta$$

$$V_a = Ri_a + L\frac{di_a}{dt} + M\frac{d(-i_a)}{dt} + E_a + \Delta$$

After simplifying above expression, we get:

$$V_a = Ri_a + L\frac{di_a}{dt} - M\frac{di_a}{dt} + E_a + \Delta$$

After re-arranging math sign and taking i_a term as common in above expression, it is expressed as:

$$V_a = Ri_a + (L - M)\frac{di_a}{dt} + E_a + \Delta \tag{3.8}$$

After modifying Eq. 3.1, we got a more realistic expression of voltage of BLDC motor as given by Eq. 3.8. The expression is now simplified into a single current and is only dependent on the current of the respective phase. This expression is used in modeling of BLDC motor and also for controller design where required.

Taking mutual induction as common term and substituting Eq. 3.6 in Eq. 3.2, we get:

$$V_b = Ri_b + L\frac{di_b}{dt} + M\frac{d(i_a + i_c)}{dt} + E_b + \Delta$$

After simplifying above expression, we get:

$$V_b = Ri_b + L\frac{di_b}{dt} + M\frac{d(-i_b)}{dt} + E_b + \Delta$$

After re-arranging math symbols and taking i_b term as common in above expression, it is expressed as:

$$V_b = Ri_b + L\frac{di_b}{dt} - M\frac{di_b}{dt} + E_b + \Delta$$

For more accurate modeling of the BLDC motor, the voltage equation of phase-B represented by Eq. 3.2 is modified and the new equation is represented by Eq. 3.9.

$$V_b = Ri_b + (L - M)\frac{di_b}{dt} + E_b + \Delta \tag{3.9}$$

Similarly, the mutual inductance is taken as common term and Eq. 3.7 is used in Eq. 3.3. As a result, the modified expression is given as:

$$V_c = Ri_c + L\frac{di_c}{dt} + M\frac{d(i_a + i_b)}{dt} + E_c + \Delta$$

After simplifying above expression, we get:

$$V_c = Ri_c + L\frac{di_c}{dt} + M\frac{d(-i_c)}{dt} + E_c + \Delta$$

After re-arranging math symbols and taking i_c term as common in above expression, it is expressed as:

$$V_c = Ri_c + L\frac{di_c}{dt} - M\frac{di_c}{dt} + E_c + \Delta$$

The voltage equation of phase-c given by Eq. 3.3 is modified and the new voltage equation for phase-C is expressed by Eq. 3.10.

$$V_c = Ri_c + (L - M)\frac{di_c}{dt} + E_c + \Delta \tag{3.10}$$

For controller design point of view, We have to change the equations of motor in terms of $\dot{i}$ in order to move towards observer dsign. Rearranging Eq. 3.8, we get the following expression:

$$(L - M)\frac{di_a}{dt} = -Ri_a + V_a - E_a - \Delta$$

Dividing by $L - M$ term in both sides of above expression, we get the following expression.

$$\frac{di_a}{dt} = -\frac{Ri_a}{L-M} + \frac{V_a}{L-M} - \frac{E_a}{L-M} - \frac{\Delta}{L-M} \tag{3.11}$$

Rearranging Eq. 3.9, we get the following expression:

$$(L-M)\frac{di_b}{dt} = -Ri_b + V_b - E_b - \Delta$$

To simplify the above expression, we have to divide $L - M$ term on both sides of the above expression, we get the following expression.

$$\frac{di_b}{dt} = -\frac{Ri_b}{L-M} + \frac{V_b}{L-M} - \frac{E_b}{L-M} - \frac{\Delta}{L-M} \tag{3.12}$$

Similarly, Eq. 3.10 can be re-written as:

$$(L-M)\frac{di_c}{dt} = -Ri_c + V_c - E_c - \Delta$$

$$\frac{di_c}{dt} = -\frac{Ri_c}{L-M} + \frac{V_c}{L-M} - \frac{E_c}{L-M} - \frac{\Delta}{L-M} \tag{3.13}$$

3.3 Sliding Mode Observer Design

The idea here is to estimate the back-EMF using the phase currents and voltages as input of the observer. We want to observe a total of 6 outputs which consist of three current variables and three back-EMF variables. The standard form of error equations for observer are:

$$\tilde{x} = x - \hat{x} \tag{3.14}$$

$$\frac{d\tilde{x}}{dt} = \frac{dx}{dt} - \frac{d\hat{x}}{dt}$$

The observer equations can be written using the stator current equations of motor as given below:

$$\frac{d\hat{i_a}}{dt} = -\frac{R\hat{i_a}}{L-M} + \frac{V_a}{L-M} + \frac{k\,\mathrm{sign}\,(\tilde{i_a})}{L-M} \tag{3.15}$$

In Eq. 3.15:

The term $k\,\mathrm{sign}\,(\tilde{i_a})$ is the switching term of the sliding mode observer and k is the gain of the observer. We can see that the estimation depends upon phase-current and phase voltage. Also, it is necessary to discuss that the Signum function depends upon current error. So, we can say that the estimation design depends upon the stator currents.

$$\frac{d\hat{i_b}}{dt} = -\frac{R\hat{i_b}}{L-M} + \frac{V_b}{L-M} + \frac{k\,\mathrm{sign}\,(\tilde{i_b})}{L-M} \tag{3.16}$$

The second equation of the observer is given by Eq. 3.16. It mainly depends upon phase current, phase voltage and the observer switching term of phase-B.

$$\frac{d\hat{i_c}}{dt} = -\frac{R\hat{i_c}}{L-M} + \frac{V_c}{L-M} + \frac{k\,\mathrm{sign}\,(\tilde{i_c})}{L-M} \tag{3.17}$$

Similarly, the third equation for phase-c is given by Eq. 3.17. Above mentioned three equations of observer are complete and the next step is to check the convergence of the error.

3.3.1 Error Convergence Analysis

In order to get the error equation for phase-a we need to subtract Eq. 3.11 from Eq. 3.15. The resultant expression is:

$$\frac{di_a}{dt} - \frac{d\hat{i_a}}{dt} = -\frac{R(i_a - \hat{i_a})}{L-M} - \frac{E_a}{L-M} - \frac{k\,\mathrm{sign}\,(\tilde{i_a})}{L-M} - \frac{\Delta}{L-M}$$

$$\frac{d\tilde{i_a}}{dt} = -\frac{R\tilde{i_a}}{L-M} - \frac{E_a + k\,\text{sign}\,(\tilde{i_a})}{L-M} - \frac{\Delta}{L-M} \tag{3.18}$$

The error equation for phase-A current is represented as:

$$e = i_a - \hat{i_a} \tag{3.19}$$

Sliding Surface:

$$S = e \tag{3.20}$$

Rewriting Eq. 3.18 in the form of error (e), we get:

$$\dot{e} = -\frac{Re}{L-M} - \frac{E_a}{L-M} - \frac{k\,\text{sign}\,(e)}{L-M} - \frac{\Delta}{L-M} \tag{3.21}$$

Using the following conditions in Eq. 3.21, we can check the stability of the system.

TABLE 3.1: Error Convergence

Condition	**Outcome**
if $e > 0$	$\dot{e} < 0$
if $e < 0$	$\dot{e} > 0$

Using above conditions in Eq. 3.21, we get the following result:

$$e\dot{e} < 0$$

Hence, the system is stable.

Now, we need to define the back-EMF estimation equation.

In Eq. 3.21, if: $k > |E_a + \Delta|$, then: $\tilde{i_a} \to 0$

As a result, $\dot{\tilde{i_a}}$ is assumed to be zero and we get the following expression:

$$0 = -\frac{E_a + k\,\text{sign}\,(\tilde{i_a})}{L-M} - \frac{\Delta}{L-M}$$

$$0 = \frac{-E_a - k\,\text{sign}\,(\tilde{i_a}) - \Delta}{L - M}$$

$$0 = -E_a - k\,\text{sign}\,(\tilde{i_a}) - \Delta$$

$$E_a = -k\,\text{sign}\,(\tilde{i_a}) - \Delta \tag{3.22}$$

We can see that the back-EMF estimation depends upon the SMO switching term and the unmodeled dynamics of the motor. We can write the above expression in terms of Signum function:

$$k\,\text{sign}\,(\tilde{i_a}) = -E_a - \Delta \tag{3.23}$$

By applying the same design steps, the equations for EMF of phase-B and phase-C can be written as:

$$E_b = -k\,\text{sign}\,(\tilde{i_b}) - \Delta \tag{3.24}$$

$$E_c = -k\,\text{sign}\,(\tilde{i_c}) - \Delta \tag{3.25}$$

3.4 Key Advantages of Our Proposed Design

Following are some of the key advantages of our proposed design:

1. Simple algorithm of SMO as compared to complex algorithms used in previous research [14].
2. No transformations of the signals are required as done in previous literature, e.g., Clarke and Park Transformations [12].
3. Use of less costly voltage/current as compared to costly hall sensors in case of hardware implementation.

3.5 Summary

Different techniques have been used in previous research in order to estimate back-EMF and to control the three-phase sensorless Brushless DC motor. One of these techniques is a Sliding Mode Observer (SMO). A simple SMO is designed using Signum function. Modeling of the BLDC is also done using its equivalent circuit. The motor model is compared with previously accepted research in order to verify the accuracy of the model. Differential equations were used to design the observer in the time domain. Currents and Back-EMF differential equations are defined along with the error signal expression. In the end, the back-EMF estimation expression is derived. This error expression depends upon the sliding mode observer gain the switching term of the observer. The implementation of the observer in MATLAB/Simulink is discussed in the next Chapter 4.

Chapter 4

Implementation of Back-EMF Estimation in MATLAB/Simulink

4.1 Introduction

The simulation of the proposed design is done in MATLAB/Simulink. Simulink is a widely used tool for simulation purposes in different areas.

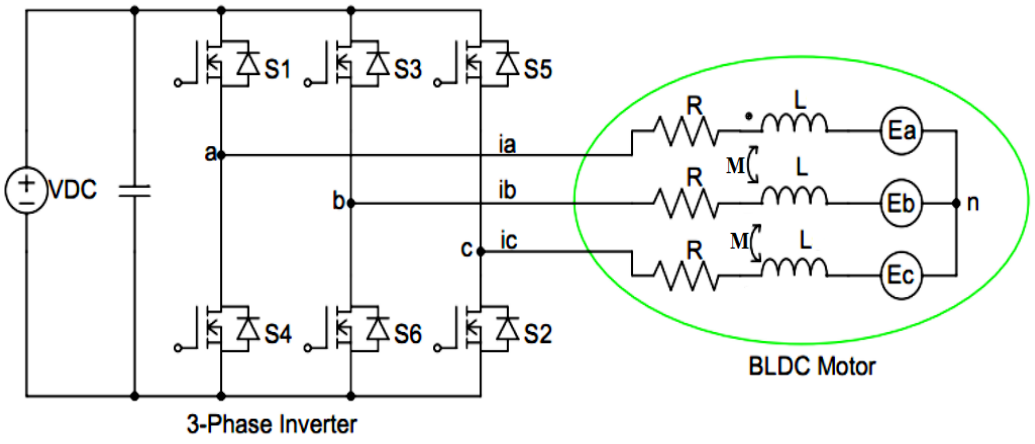

FIGURE 4.1: BLDC Motor Drive Representation [8]

Fig. 4.1 represents a BLDC Motor drive system that has a three-phase inverter at the front end. In our implementation, the six input signals that are supplied to the motor are the outputs of inverter. The connections of the three phases of

the inverter with the motor are also shown in the figure. We have additionally implemented a complete BLDC drive system which includes three-phase inverter. Three Ammeters and three Voltmeters are required at point a,b and c in order to supply input to the designed observer. We have used S-function to implement the observer equations derived in chapter-3. For input/output and results display, a Simulink model is created. Let us discuss the complete BLDC motor drive first because it is important to understand the whole picture regarding design point of view before moving towards our specific part of the research. The details of the design are further discussed in the upcoming sections of this chapter.

4.2 Overview of Brushless DC Motor Control Using MATLAB/Simulink

Our main focus in this research is to design an observer for estimation of the back-EMF signal which can be further used to generate the commutation sequence for inverter in order to run the BLDC motor. But first, we need to understand how the overall BLDC drive system works, from where we will get the input for our observer and what are the necessary components that are required to implement the observer.

A BLDC motor control system is implemented in MATLAB/Simulink shown in Fig. 4.2. The motor is implemented using a Simulink block for the motor shown in green color. The rotor position is used to determine the reference currents of three phases which are supplied to the current controller(subsystem1). Because the BLDC motor has an electronic commutation, so, the current controller generates the switching signals for the inverter. A PID controller is also implemented for speed tracking of the motor [16].

Another implementation of BLDC motor drive system based on hall sensor is shown in Fig. 4.3. The motor is implemented using Simulink block for the motor shown in orange color. Hall sensors are used to get the position of the rotor.

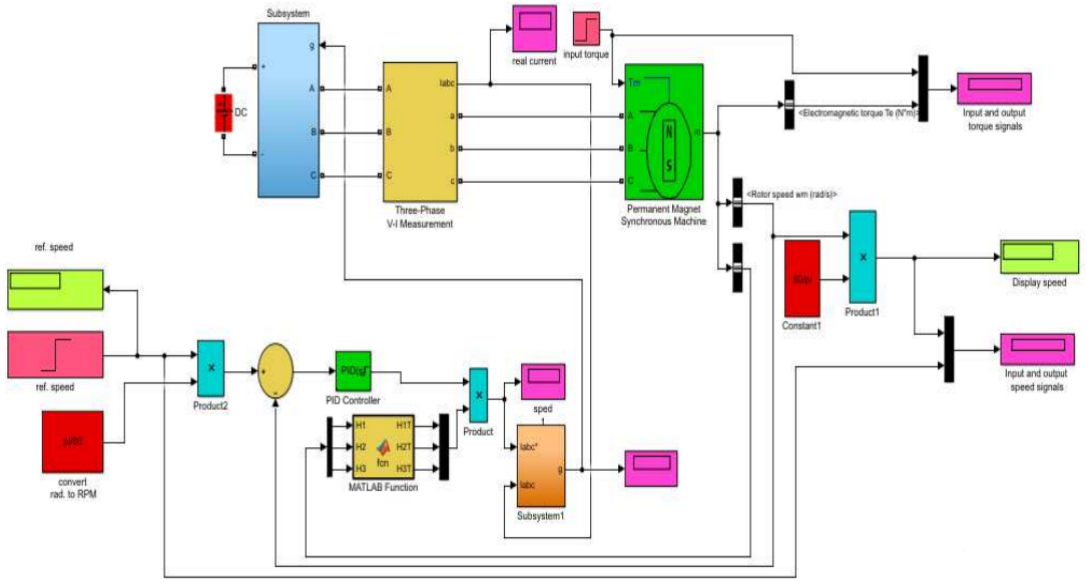

FIGURE 4.2: BLDC Motor Control Implementation in Simulink [16]

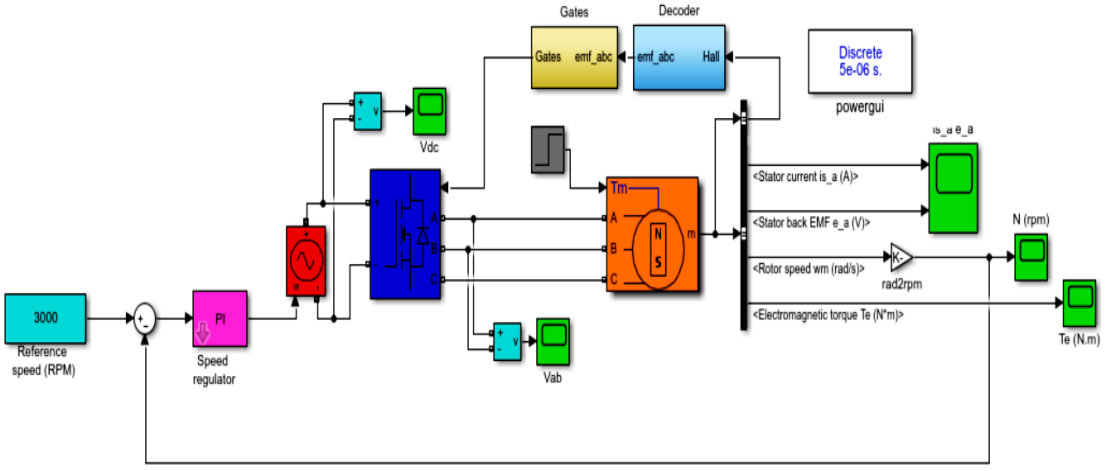

FIGURE 4.3: BLDC Motor Drive System [17]

This position is then used to determine the EMF signals. EMF signals are used to generate the commutation sequence for the inverter switches. There are six switches for the switching of three-phase BLDC motor. A speed controller is implemented like a PI speed controller for speed tracking. Reference speed (rpm) is provided as input. Subtractor has generated the error between reference speed and actual speed which is fed to PI controller. The control input is attached to BLDC motor phase through a controlled voltage source.

Keeping in mind the systems shown in Fig. 4.2 and Fig. 4.3, BLDC drive system has following main components:

1. BLDC Motor
2. Three Phase Inverter
3. Gating Signal Generator
4. Speed Controller

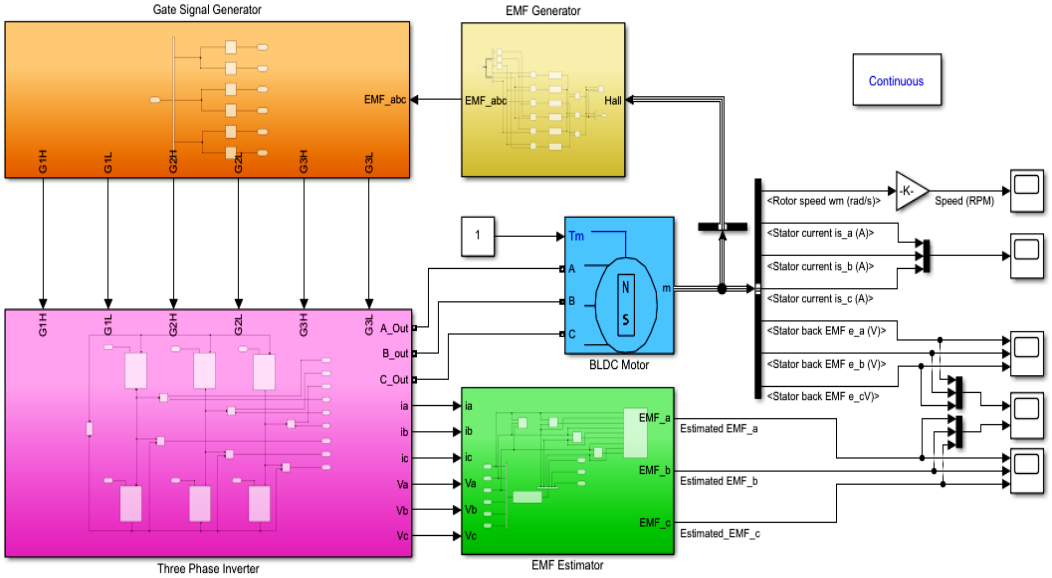

FIGURE 4.4: Our Implementation of BLDC Motor Drive

Moving towards out implementation, all the essential components are integrated to implement the overall BLDC drive in MATLAB/Simulink as shown in Fig. 4.4. Hall sensors detect the rotor position which is used to determine the back-EMF. EMF signals are then fed to the gate signals generator which generates switching signals for the inverter operation. A sliding mode observer is also shown. We will discuss the observer model design in detail in the next section of this chapter. For Now, the main idea of a BLDC Motor control system is clear, let us discuss some of the above mentioned components in order to comprehend the motor operation and control.

4.2.1 BLDC Motor

Simulink has a block of "Permanent Magnet Synchronous Machine" which can be used as BLDC Motor if the back-EMF waveform setting is set to trapezoidal

instead of sinusoidal. The Simulink block is shown in Fig. 4.5. We have already discussed in Chapter 2 that the BLDC motor has a trapezoidal shape of back-EMF waveform. This motor block has three phase input and a mechanical torque input. There are multiple outputs of this block.

We have given the motor model equation in Chapter 3 and we have used this block in our proposed Simulink model.

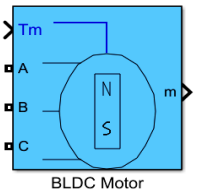

FIGURE 4.5: Siumulink Block for BLDC Motor

4.2.2 EMF Detection/Estimation

TABLE 4.1: EMF Table [18], [19]

H_a	H_b	H_c	E_a	E_b	E_c
0	0	0	0	0	0
0	0	1	0	-1	+1
0	1	0	-1	+1	0
0	1	1	-1	0	+1
1	0	0	+1	0	-1
1	0	1	+1	-1	0
1	1	0	0	+1	-1
1	1	1	0	0	0

A general implementation of BLDC motor control has hall sensors for sensing rotor position. One way is to generate Back-EMF using these hall sensor values as inputs. There are three hall sensors mounted on the stator of BLDC motor. These sensors are 120° apart from each other. These sensors work on the basis of Hall Effect theory that is discussed in Chapter 1. There is three digit output for every 60° as the hall sensors sense the current and the respective back-EMF signal is decoded using the Table 4.1. This table is used for BLDC motors with hall sensors.

In our proposed design, we are using sensorless BLDC motor. We have estimated back-EMF using a sliding mode observer (SMO) as discussed previously.

4.2.3 Gating Signal Generator

TABLE 4.2: Commutation Sequence Table [18], [19]

E_a	E_b	E_c	S_1	S_2	S_3	S_4	S_5	S_6
0	0	0	0	0	0	0	0	0
0	-1	+1	0	0	0	1	1	0
-1	+1	0	0	1	1	0	0	0
-1	0	+1	0	1	0	0	1	0
+1	0	-1	1	0	0	0	0	1
+1	-1	0	1	0	0	1	0	0
0	+1	-1	0	0	1	0	0	1
0	0	0	0	0	0	0	0	0

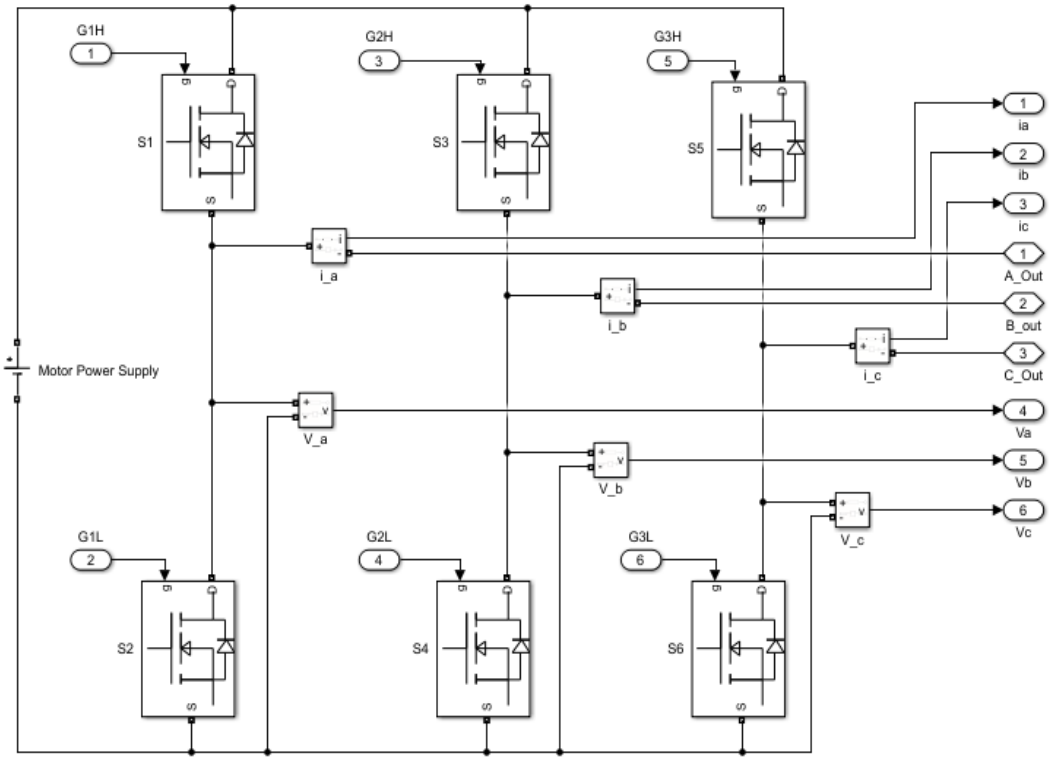

FIGURE 4.6: Three-Phase Inverter Model

The back-EMF Table 4.1 gives three-digit output for a three-digit combination of hall sensors data. The switching pattern for the inverter can be generated using

Table 4.2. '1' means the switch in ON and '0' means the switch is OFF. The inverter has three legs. Each leg has two switches. In this case, Metal Oxide Semiconductor Field Effect Transistor (MOSFET) is used as a switch. There is a high side switch and a low side switch on each leg. There are total six switches as mentioned in Table 4.2. S_1 means switch number 1. Using this pattern the six sequences are generated. For every 120°, one switch is fully ON. For every 60°, one high side switch from one leg and a low side switch from another leg are ON. The remaining third leg is disconnected in this case. We have made a model of a three-phase inverter in Simulink as shown in Fig. 4.6. Total six switches are shown with their label. Here, we can clearly see that the inverter has six sensors, three for voltage measurement and three for current measurement. All six outputs are used for observer design.

4.3 S-Function Implementation in MATLAB

An ***S-function*** is an implementation of a Simulink block that is written in MATLAB using C, C++ or other languages. An algorithm can be implemented using simple set of rules and the function can be called in Simulink using the "S-Function" block from the Simulink library. The name of the S-function must be defined in the block before running the model [20].

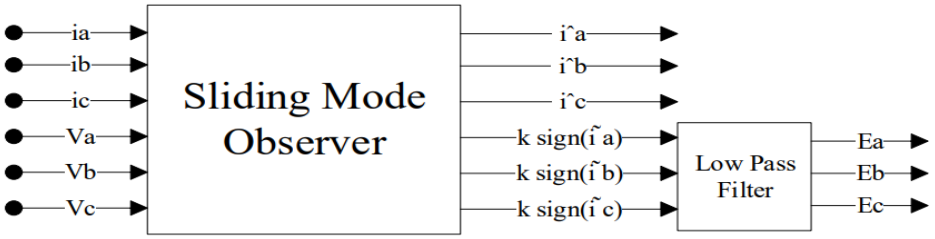

FIGURE 4.7: Observer Implementation

Fig. 4.7 represents the implementation of the designed Sliding Mode Observer in MATLAB/Simulink. The first three inputs are the currents of the three phases of the BLDC motor. The remaining three inputs of SMO are the three input voltages of BLDC motor. Here you can see that the S-function estimates three

phase currents and three current error functions on the basis of the six input signals. The variable k represents the sliding mode controller gain. A Low pass filter is used to filter out our required three back-EMF of the BLDC motor.

4.3.1 S-function Parameters/Arguments Details

S-function implementation in MATLAB requires the following three main arguments:

1. Sample Time (t)
2. State Vector (x)
3. Input Vector (u)

The next step is the initialization of the variables and the initial states in the S-function. Table 4.3 shows the name and size of the variables/vectors used.

TABLE 4.3: S-Function Parameter's Size Initialization

SN	Parameter	Size
1	Continuous States	6
2	Inputs	6
3	Outputs	6

Following are the six inputs of the S-function:

1. Phase-A Current (i_a)
2. Phase-B Current (i_b)
3. Phase-C Current (i_c)
4. Phase-A Voltage (V_a)
5. Phase-B Voltage (V_b)
6. Phase-C Voltage (V_c)

Similarly, the six output signals of the S-function are:

1. Estimated Phase-A Current ($\hat{i_a}$)
2. Estimated Phase-B Current ($\hat{i_b}$)
3. Estimated Phase-C Current ($\hat{i_c}$)
4. Estimated Phase-A Back-EMF (e_a)
5. Estimated Phase-B Back-EMF (e_b)
6. Estimated Phase-C Back-EMF (e_c)

4.3.1.1 BLDC Motor Specifications in S-Function

Other important parameters to be defined and initialized are the electrical specification of the motor. Table 4.4 shows the specifications of the BLDC motor which are required to implement motor equations in the S-function.

TABLE 4.4: Motor Specifications in S-Function

SN	Parameter	Value
1	Voltage	48 V
2	Stator Phase Resistance (R)	0.5 Ω
3	Stator Phase Inductance (L)	1.5×10^{-3} H
4	Mutual Inductance (M)	0.15×10^{-3} H

4.3.1.2 Differential Equations Implementation

Moving towards the implementation of the differential equation of the motor and the observer in S-function. A total of six differential equations are written in MATLAB. The first three equations are of the phase current estimation. Let us discuss the equations of Phase-A written in MATLAB.

Fig. 4.8 represents the implementation of observer current error in MATLAB S-function as mentioned in the observer error equation Eq. 3.14. The sliding mode

```
i_a_tilde=i_a-i_a_hat; % observer state error
```

FIGURE 4.8: Current Error Equation

observer needs both inputs (phase current i_a and its estimate $\hat{i_a}$) for current error generation. So, we have supplied the input current from the inverter output. For the estimation of current, we have written a differential equation as discussed in the observer design section.

We can clearly see that the expression shown in Fig. 4.9 which is implemented in MATLAB is same as observer design Eq. 3.15.

```
i_a_hat_dot=(1/(L-M))*(-R*i_a_hat+V_a+neu_a); % observer equation
```

FIGURE 4.9: Observer Equation for Phase-A Current

Here, neu_a is the variable that is the sliding mode observer term. The implementation of this term in MATLAB is shown in Fig. 4.10.

```
neu_a=k*sign(i_a_tilde);
```

FIGURE 4.10: Observer Term

The complete set of currents and error equations as written for phase-A in MATLAB are also written for the remaining phase-B and phase-C as well. The EMF estimation design equation for phase-A mentioned in Eq. 3.22 is written in MATLAB as shown in Fig. 4.11.

```
e_a=-neu_a-delta;
```

FIGURE 4.11: EMF Estimation Equation

The transfer function of low pass filter can be written as:

$$Y = \left(\frac{p}{s+p}\right) U$$

Here, $p = 2\pi f$ is the cut-off frequency of the low pass filter in rad/sec.

Y is the output

U is the input

In our case, we need to have a differential equation of the filtering signal in order to implement it in S-function. Therefore, we need to convert the expression into the time domain. This can be done using the inverse Laplace transform. By taking the inverse Laplace transform of the transfer function of LPF, we can re-write the above expression in the time domain in a following way:

$$\dot{y} = -py + pu \tag{4.1}$$

Eq. 4.1 is written in MATLAB to filter out the required back-EMF. Let us consider only phase-A, We need to apply LPF on e_a. So, the input signal u can be expressed as:

$$u = e_a$$

Using above expression in Eq. 4.1, we get the following expression of the LPF.

$$\dot{y} = -py + pe_a \tag{4.2}$$

By writing the code of Eq. 4.2 in S-function, the back-EMF signals of all the phases are filtered out. The implementation of the back-EMF differential equation in MATLAB for phase-A is shown in Fig. 4.12.

```
e_a_dot=-p*x(4)+p*(e_a);
```

FIGURE 4.12: Differential Equation of EMF

Here, p is the cut-off frequency of the filter in rad/sec. $x(4)$ means the fourth state in the state vector. The fourth state is the estimation of back-EMF of phase-A which is also the required output in our observer design. Similarly, the differential equations of back-EMF of remaining phase-B and phase-C are also written in MATLAB.

```
sys = [i_a_hat_dot i_b_hat_dot i_c_hat_dot e_a_dot e_b_dot e_c_dot];
```

FIGURE 4.13: Complete System Representation in S-Function

As the observer design has six outputs, so, the complete system in S-function has six differential equations as shown in Fig. 4.13. First three equations are the derivatives of current estimation and the remaining three are the derivatives of back-EMF of all phases.

4.4 Observer Simulink Model Design

The calling of S-function and the display of input and output signals is implemented in Simulink. Let us discuss the Simulink model design in detail in this section.

4.4.1 Required Simulink Library Blocks

In order to call the S-function and display the required results, some commonly used Simulink blocks were added to model and attached accordingly. The list of the blocks used is mentioned in Table 4.5.

TABLE 4.5: List of Simulink Library Blocks

SN	Block Name
1	S-function
2	Inport
3	Outport
4	MUX
5	DEMUX
6	Subtract
7	Scope

4.4.2 Construction of the Simulink Model after S-Function Design

The Simulink blocks mentioned in Table 4.5 were added to the model and then connected to each other as shown in Fig. 4.14. Let us discuss the construction of

this model and the purpose of blocks used. Inport blocks are used to get the input signals from inverter block.

First three inport blocks are used to supply current inputs and the remaining three were used to supply voltage signals of three phases. A Multiplexer (MUX) was used to merge all input signals into a vector and then feed it to the observer S-function as shown. The are a total of six signals as mentioned in the previous section.

S-function algorithm is written in MATLAB. To call that function, a Simulink library block named "S-Function" is added to model. To run the S-function in Simulink, the name of the function must be defined in the "S-function" block. It was done by double clicking the block and writing the desired name in block parameter setting window.

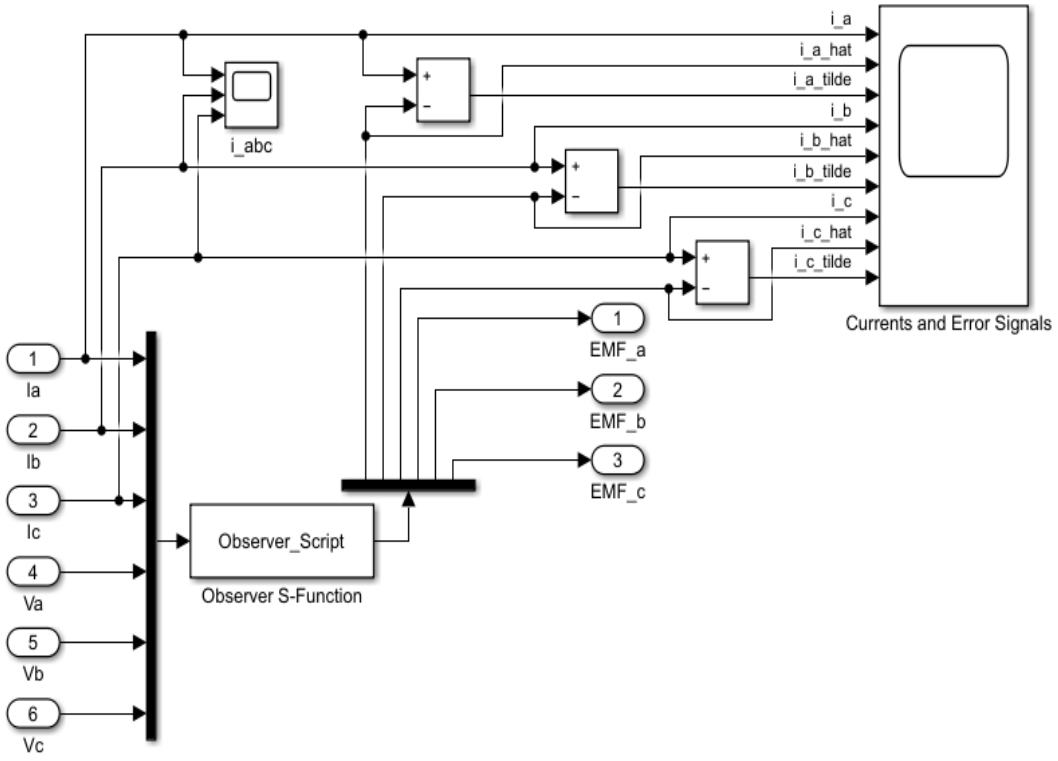

FIGURE 4.14: Observer Simulink Model

The output of the MUX was connected to the observer input and its output was connected to a Demultipltxer (DEMUX). The DEMUX was sued to to extract the required signals from the output vector of the S-function. There are a total of six output signals which are also mentioned in previous section of this Chapter.

To generate the error signals of currents, Eq. 3.14 was implemented in Simulink model. As you can see in Fig. 4.14, the first three signals i_a, i_b and i_c from the inports are subtracted from $\hat{i_a}, \hat{i_b}$ and $\hat{i_c}$ respectively to get $\tilde{i_a}, \tilde{i_b}$ and $\tilde{i_c}$ error signals.

For subtraction, subtract block was used for all three phases.

The remaining three signals from the output of the S-function block are the required estimated back-EMF outputs. These signals are fed to the main Model using the outport block from library. These signals are displayed in the main model.

Scope block was used to display all signals for a specified simulation time that can be modified from the Simulink model settings.

4.5 Summary

There are different tools available to implement our proposed design. We have selected MATLAB/Simulink for this purpose. MATLAB is a powerful and widely used tool to implement or simulate different problems from different fields. BLDC motor is modeled and the Sliding Mode Observer (SMO) for back-EMF estimation is designed after a detailed survey and analysis of the best possible techniques to implement our proposed observer. The details of the simulation in MATLAB/Simulink and the observer estimation results are discussed in the next Chapter 5.

Chapter 5

Simulation and Results Discussion

5.1 Introduction

The Simulink model designed in Chapter 4 gives a total of six outputs. The first three outputs are the estimation results of currents and the remaining three are the estimation results of back-EMF of three phases. The main focus of this chapter will be the analysis of the estimation of back-EMF signals. The validity of the designed observer model will be discussed along with the key feature of our design approach.

5.2 Simulation Requirements

5.2.1 BLDC Motor Parameters

Fig. 4.4 has shown the BLDC motor block in blue color. To run the simulation, BLDC motor block needs some parameters to be defined. A list of the motor parameters used in the Simulink block are given in Table 5.1. These parameters are also included in the S-function design in Chapter 3.

TABLE 5.1: BLDC Motor Specifications

SN	Parameter	Value
1	Voltage	48 V
2	Stator Phase Resistance (R)	0.5 Ω
3	Stator Phase Inductance (L)	1.5×10^{-3} H
4	Pole Pairs	2
5	Inertia	2×10^{-3} kgm^2
6	Viscous Damping	4.924×10^{-5} Nms
7	Static Friction	3.42×10^{-3} Nm

5.2.2 Input Current Signals

Let us visualize the three currents that are required as input for sliding mode observer. These are the three current signals mentioned as i_a, i_b and i_c in Eq. 3.1, Eq. 3.2 and Eq. 3.3. These currents are important because our SMO estimation depends upon these currents.

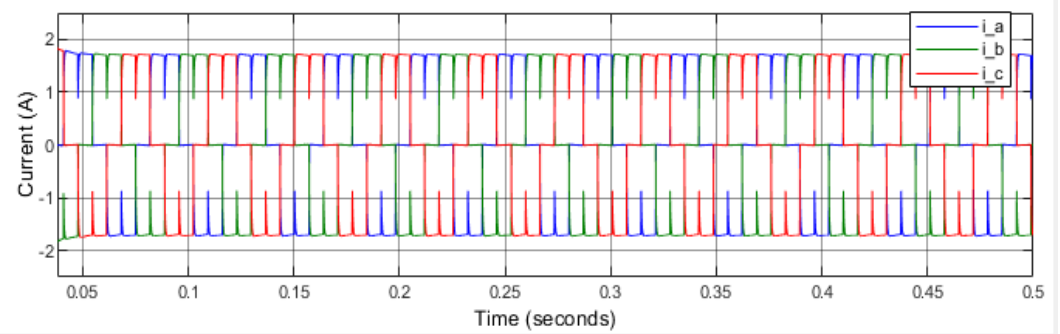

FIGURE 5.1: Input Current Signals

Fig. 5.2 provides a detailed view of the input current signals.

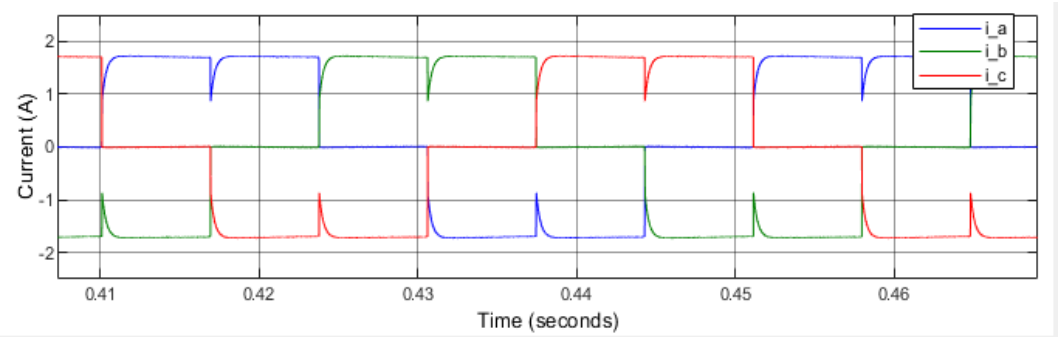

FIGURE 5.2: Input Currents Pattern

Here, you can observe the pattern and the phase difference between three phases. The color pattern mentioned in the figure legend differentiates the three signals. Another more clear view of input currents pattern can be seen in Fig. 5.3 that can be used to validate the accuracy of input currents used.

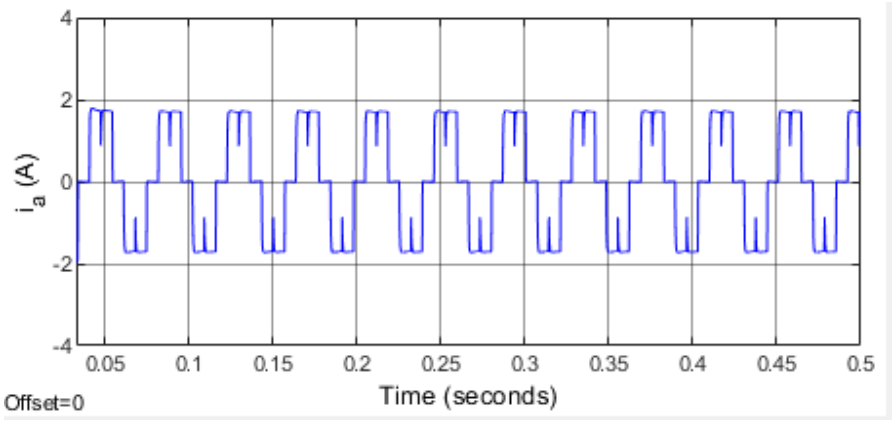

(a)

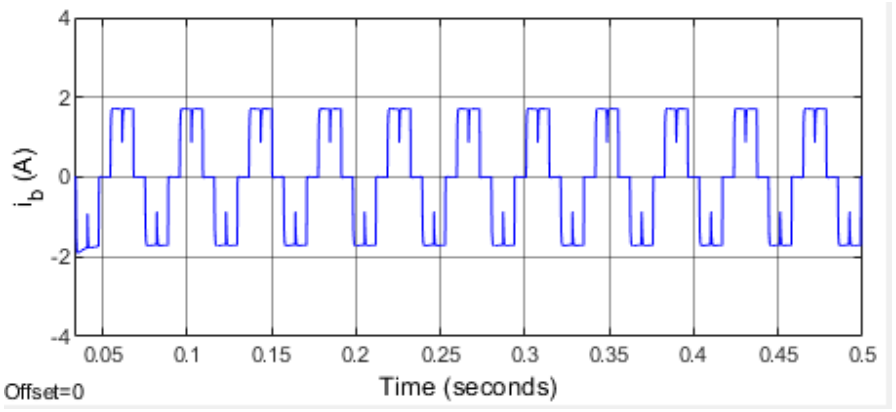

(b)

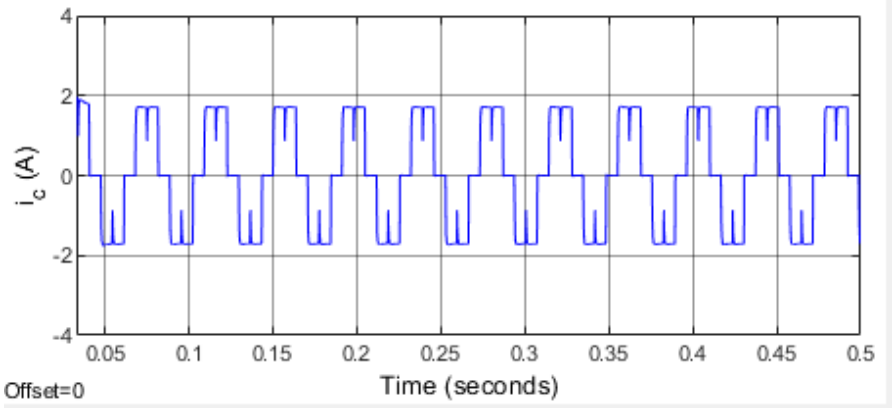

(c)

FIGURE 5.3: (a) Phase-A Stator Current (b) Phase-B Stator Current (c) Phase-C Stator Current

The input currents used are realistic and accurate and are already present in the previous research in [8] as shown in Fig. 5.4.

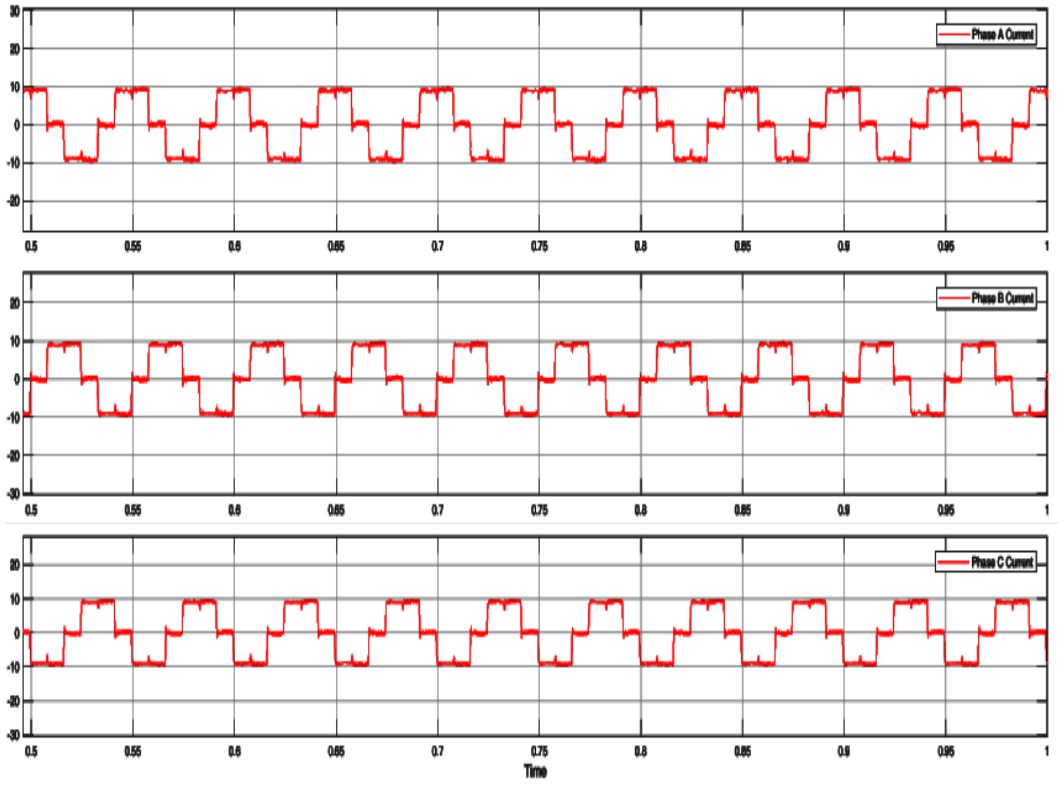

FIGURE 5.4: Reference Current Signals from Previous Research [8]

A previous research on BLDC drive Control implemented on hardware can be used as a reference to verify the accuracy of input current signals in terms of shape/pattern. The result of phase-A current using the proposed method of this research in [9] is shown in Fig. 5.5. We can see that the phase current is changing its polarity according to the switching of the inverter.

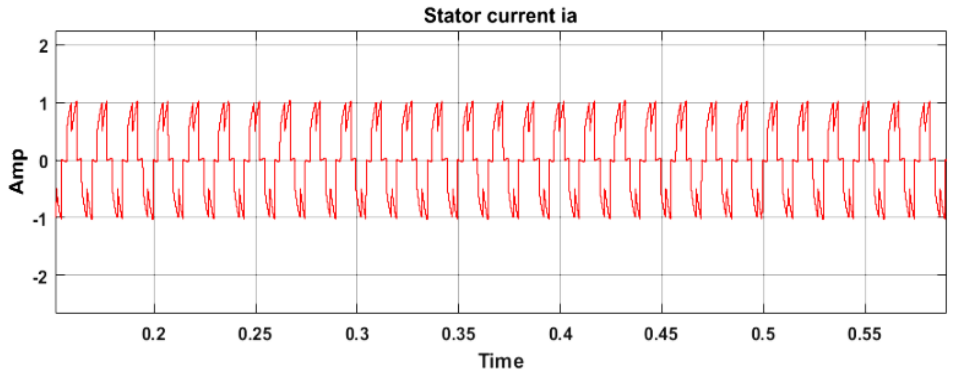

FIGURE 5.5: Phase-A Current of Proposed Method in [9]

Another research on BLDC drive Control implemented on hardware for high speed motors can be used as reference to verify the accuracy of input current signals in terms of shape/pattern. The result of phase-A current using propose method of this research in [21] is shown in Fig. 5.6.

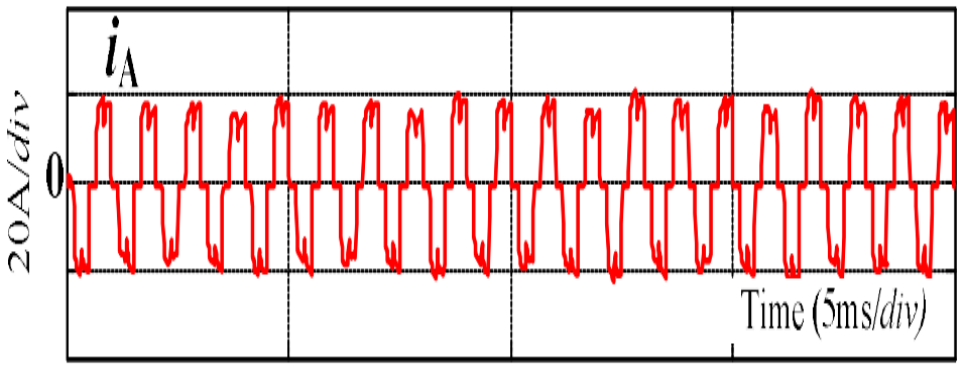

FIGURE 5.6: Phase-A Current of Proposed Method in [21]

5.3 Input Currents Estimation

The S-function implementation gives three estimation of currents. The implementation of differential equation for current estimation can be seen in Fig. 4.9. The SMO design equations for current estimation are also given by Eq. 3.15, Eq. 3.16 and Eq. 3.17 for three phases. The Back-EMF estimation design depends upon the phase currents, therefore, it is necessary to check the results of estimation of the input currents. The estimation of phase-A current can be seen in Fig. 5.7 which shows the current signal with respect to time for an interval of 0.5 seconds.

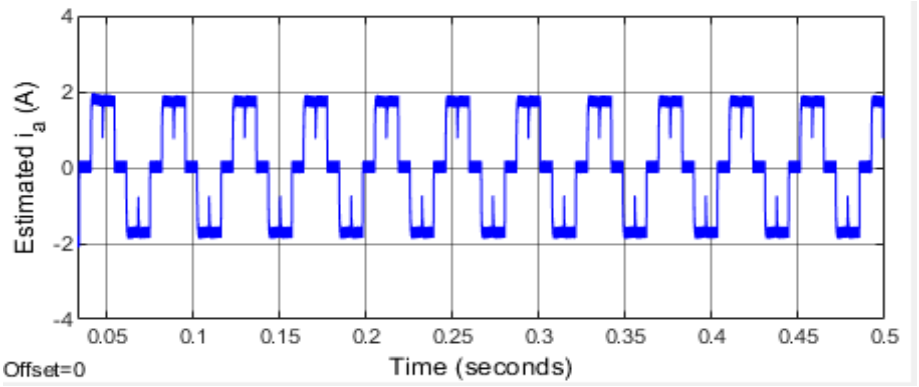

FIGURE 5.7: Estimated Phase-A Current

A complete result of all the estimated currents of all phases shown in Fig. 5.9 shows that the our designed SMO has good performance in estimating the current signals. Here, we can see that the estimation result are almost similar to the reference currents which indicates that the observer has a good estimation of both currents and EMFs. The accuracy of the input currents shown in Fig. 5.3 and the current estimation result of phase-A shown in Fig. 5.5 can be checked and verified from results of the research in [8] as shown in Fig. 5.4. Stator current results of research in [9], [21] are shown in Fig. 5.5 and Fig. 5.6 respectively for current signals verification. The comparison of all three phases can be seen in Fig. 5.9.

Our current estimation results are almost similar to previous research results. This shows that the input signals and their estimations are accurate and practical. This also proves that a sample and precise observer was proposed and implemented in our research for the estimation of the above current and EMF signals.

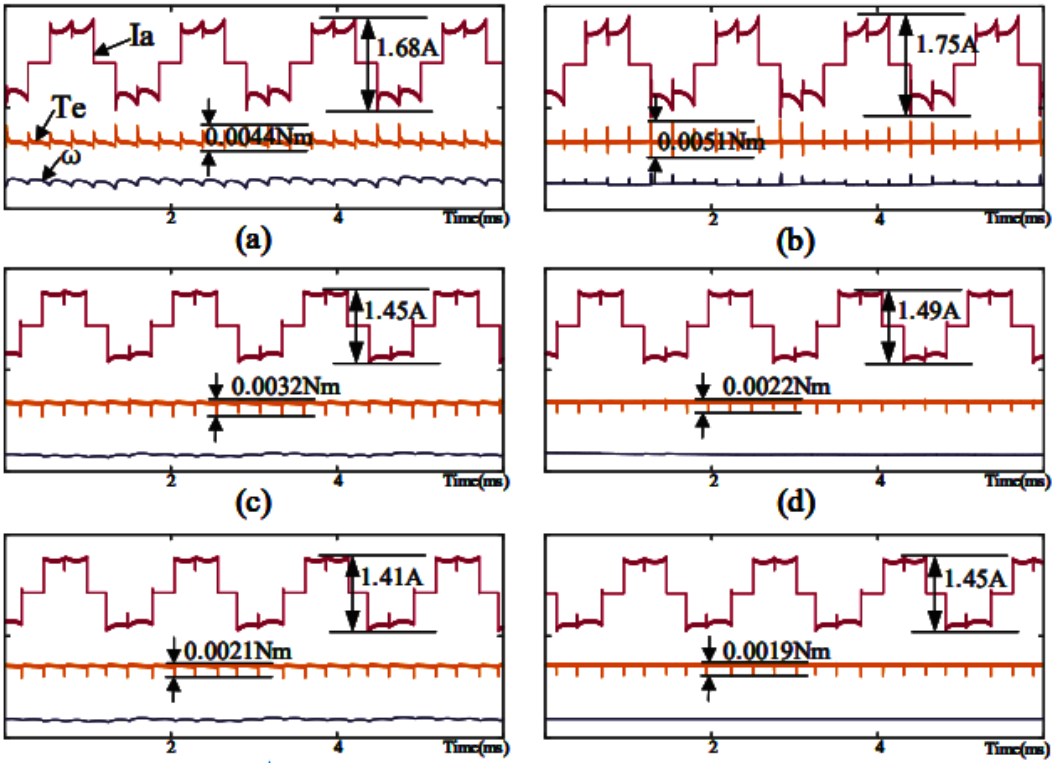

FIGURE 5.8: Reference Current Results for different methods used in [15]

The results of [15] are shown in Fig. 5.8 where the BLDC control is implemented in hardware as well can be used as a reference to check the accuracy of inputs currents used and their estimation. All the references mentioned along with their

results show the accuracy of our model. Here it is necessary to mention that the simplicity of our proposed observer has a huge effect on its performance.

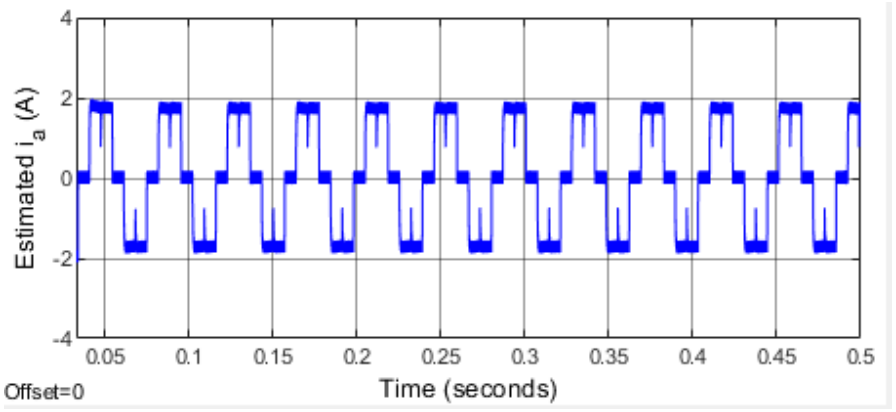

(a)

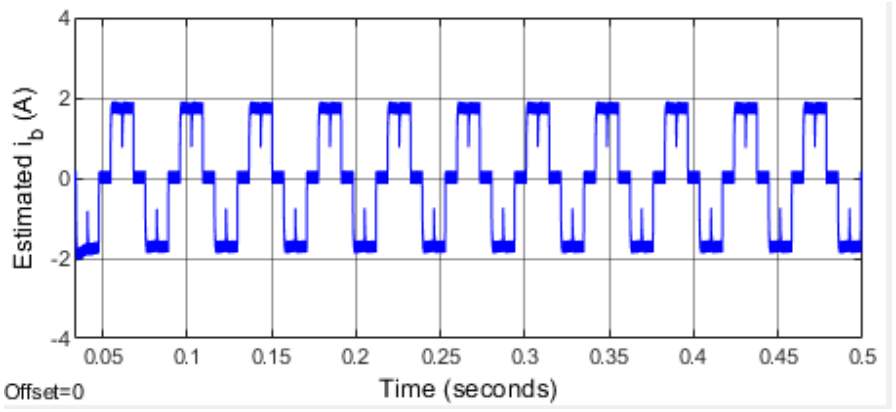

(b)

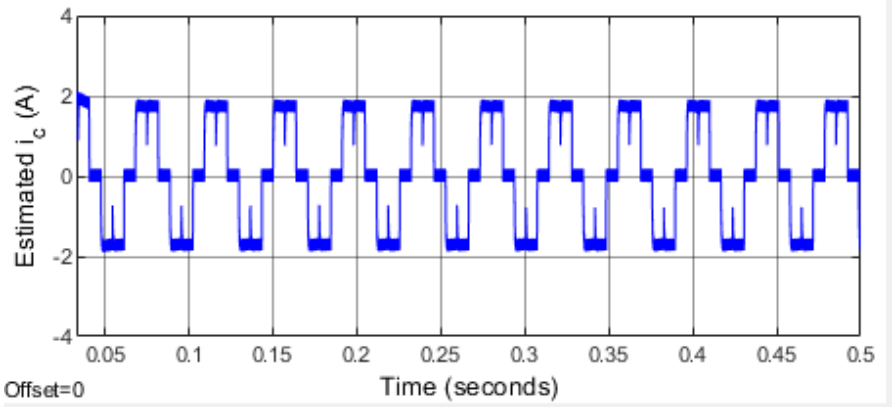

(c)

FIGURE 5.9: (a) Estimated Phase-A Current (b) Estimated Phase-B Current (c) Estimated Phase-C Current

Our designed SMO equations depend upon current signals. So, let us discuss the current error signal for all three phases.

5.3.1 Error Signal Analysis

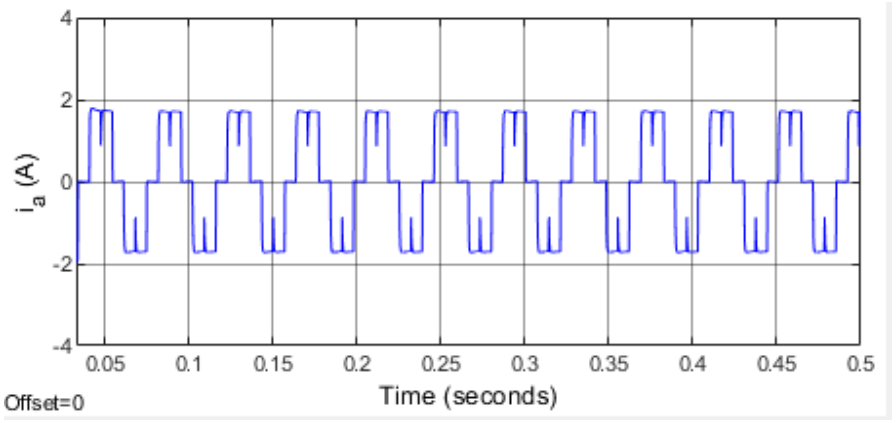

(a)

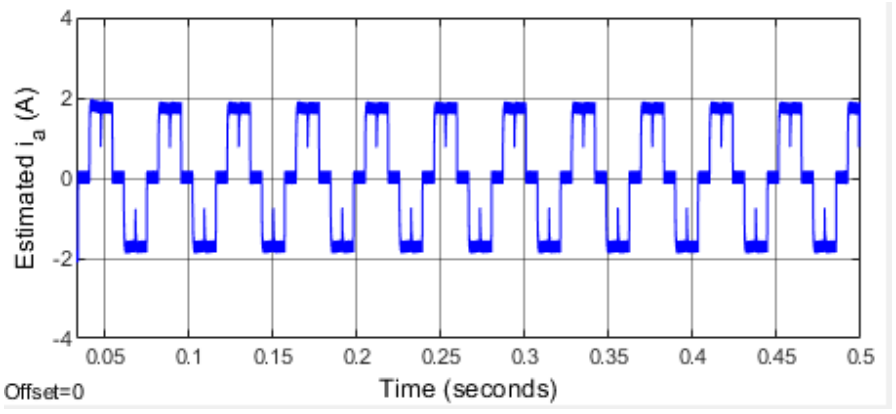

(b)

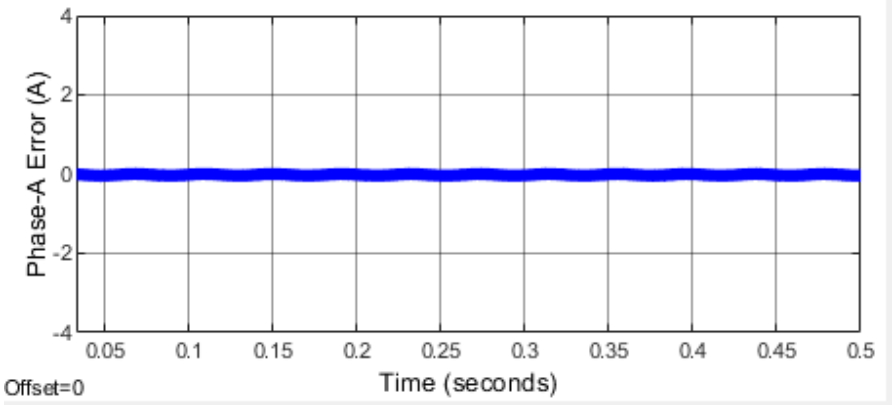

(c)

FIGURE 5.10: Error Signal Analysis for Phase-A (a) Phase-A Current (b) Estimated Phase-A Current (c) Phase-A Current Error

The comparison of phase-A input current with its estimation is shown in Fig. 5.10. The error signal shows the performance and accuracy of estimation of our designed sliding mode observer. We can see that the estimated current is almost

similar to the reference input current for phase-A. There are some oscillations in the error but the magnitude of the oscillation is negligible which also shows an optimal design of the SMO gain expression followed by Eq. 3.18.

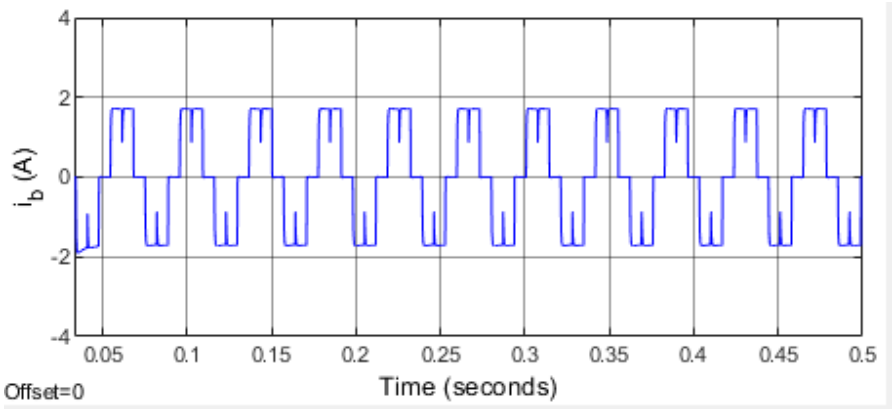

(a)

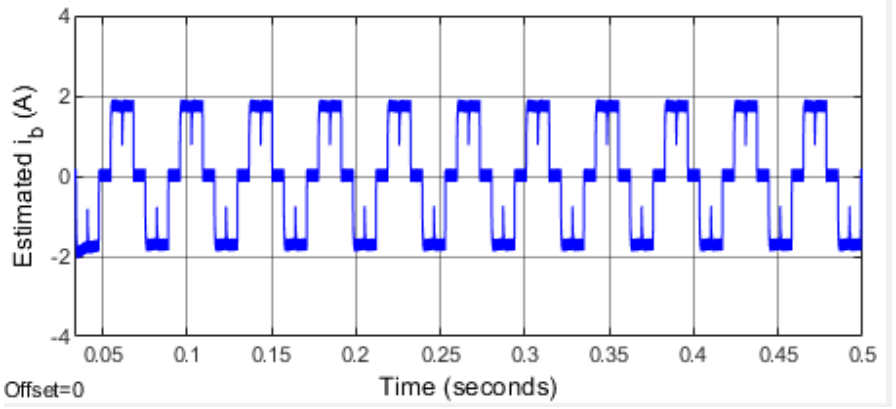

(b)

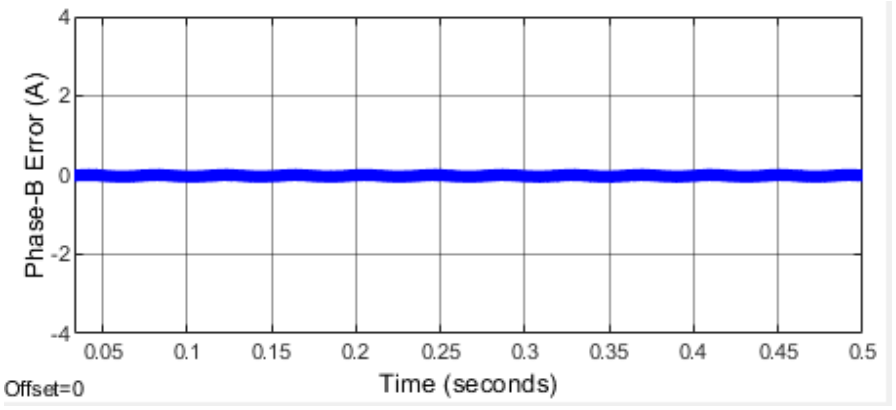

(c)

FIGURE 5.11: Error Signal Analysis for Phase-B (a) Phase-B Current (b) Estimated Phase-B Current (c) Phase-B Current Error

Fig. 5.11 shows the comparison of phase-B current with its estimation signal. There are oscillations of negligible amplitude and no phase difference can be seen.

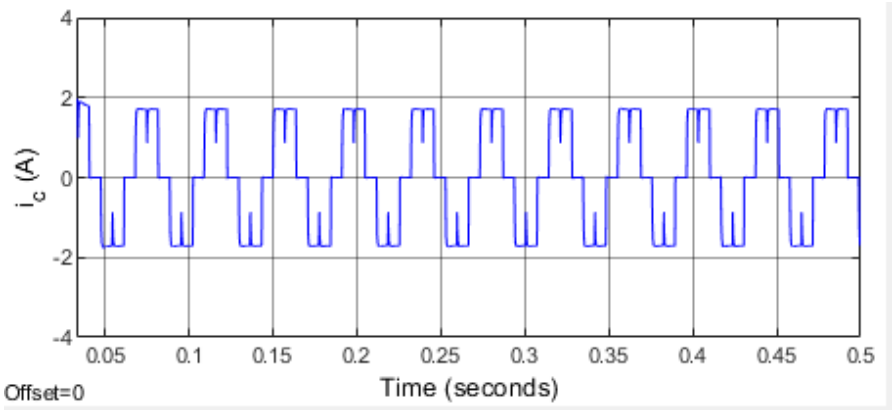

(a)

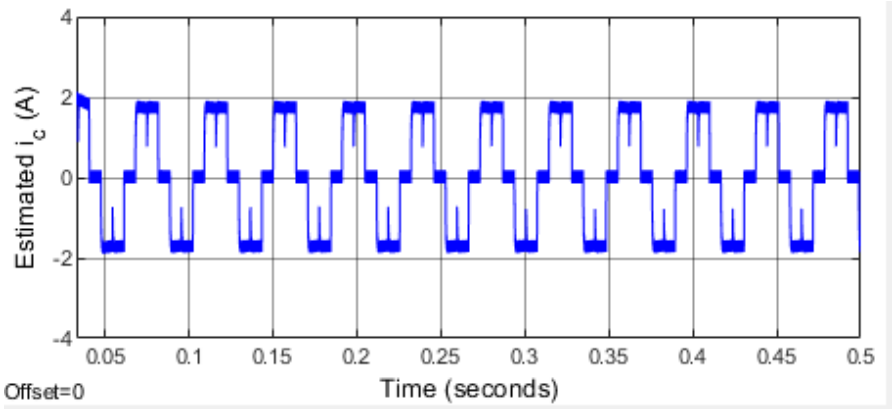

(b)

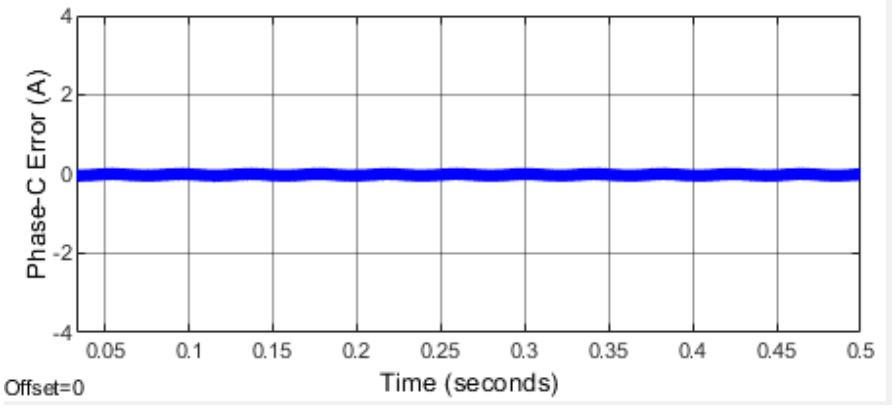

(c)

FIGURE 5.12: Error Signal Analysis for Phase-C (a) Phase-C Current (b) Estimated Phase-C Current (c) Phase-C Current Error

Similarly, Fig. 5.12 shows the comparison of phase-C input current with its estimation signal is shown. The error signal for this phase shows that the designed SMO

has good performance in currents estimation. The authenticity of the estimated current signals is already discussed with reference to previous research.

5.4 Back-EMF Estimation

The currents estimation has shown that the SMO has good performance till now. Let us discuss the estimation of back-EMF signals which is our main objective of this research. Fig. 5.13 shows the estimation of the back-EMF signals of three phases of the motor. The simulation results are shown for 0.5 seconds that were enough to achieve the steady state. Phase-A current is shown with blue color, phase-B with green color and the phase-C with red color.

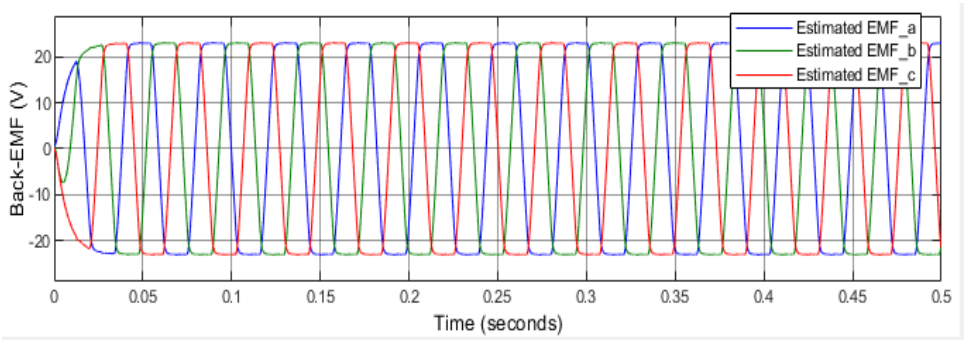

FIGURE 5.13: Estimated Back-EMF Signals

5.4.1 Analysis of Back-EMF Estimation Accuracy

The response shown in Fig. 5.14 gives a more detailed view of the estimated back-EMF signals. Here, it is necessary to analyze that shape or pattern of the estimated signals is trapezoidal which is the pattern for a BLDC motor. This result also shows that the sliding mode observer (SMO) has good performance in estimating currents as well as back-EMF signals. This also shows that the observer was accurately designed and implemented in MATLAB/Simulink.

The estimated results can be compared and their accuracy can also be verified form the results of [8], [10]. These research papers how that the back-EMF signals are trapezoidal and our estimated results are similar to their results. These results

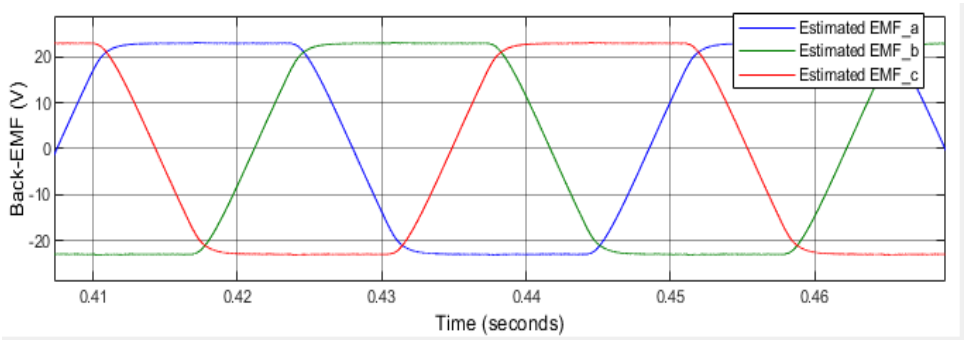

FIGURE 5.14: Detailed View of Estimated Back-EMF Signals

were used further for gate signal generation for inverter. Therefore, it is important to verify the accuracy of these results with the previous research.

The accuracy of results can also be verified from the sensorless control system implemented [9]. The research in [15], [22] shows hardware results that are more practical to compared with. This paper proposed that back-EMF signals are not ideal trapezoidal due to manufacturing and design errors, instead they lie between sinusoidal and trapezoidal waveform.

5.4.2 Comparison of Estimated Back-EMF Signals with Standard Trapezoidal Signals

Let us compare the estimated back-EMF signals with the standard trapezoidal back-EMF signals in order to analyze the performance of the sliding mode observer. Fig. 5.15 shows the comparison of estimated back-EMF signals with the standard trapezoidal back-EMF signals. The results are generated for a time of 0.5 seconds. Phase-A back-EMF is shown with blue color, phase-B with green color and phase-C with red color. We can see that the estimated back-EMF signals are similar to reference trapezoidal signals in terms of amplitude, pattern and shape of the signal. The results are also verified from the previous research mentioned and discussed in this Chapter.

Fig. 5.16 shows a more detailed view of the comparison of the back-EMF signals. We can see that the pattern of the estimated signals is almost similar to that of

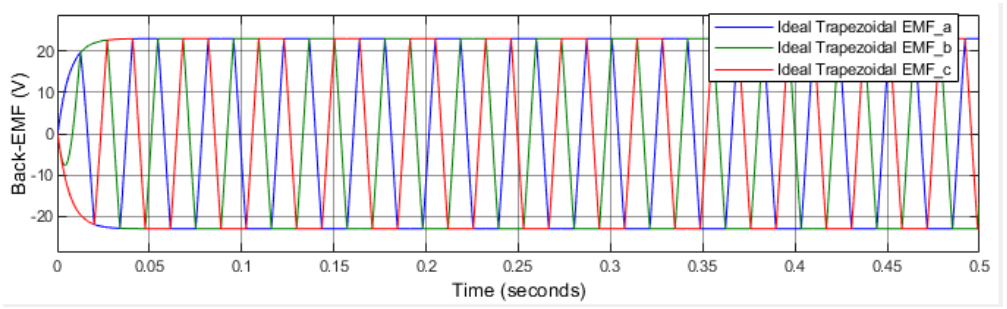

(a)

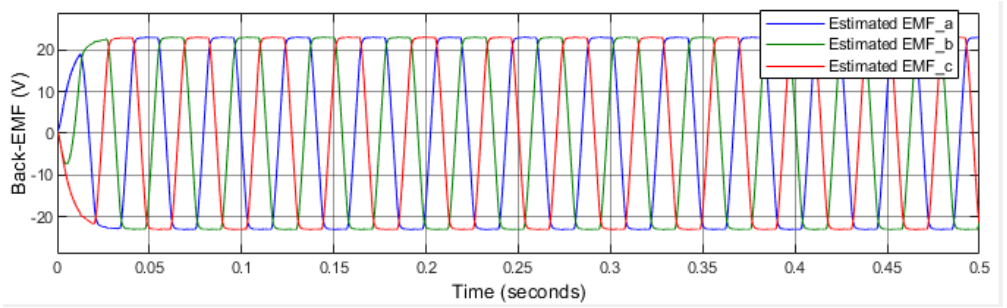

(b)

FIGURE 5.15: Comparison of Back-EMF Estimation with Ideal Back-EMF Signal a) Ideal Back-EMF Signal (b) Estimated Back-EMF Signal

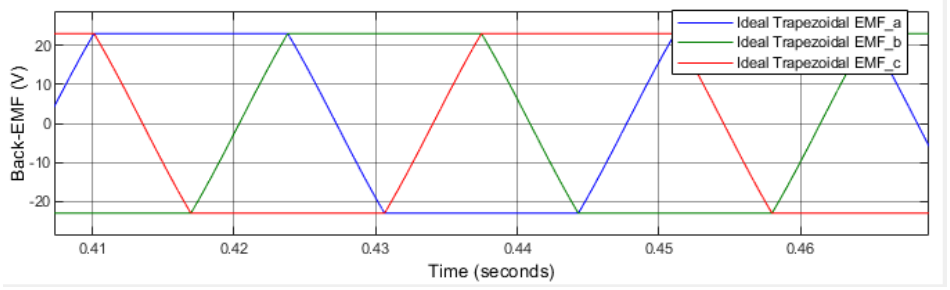

(a)

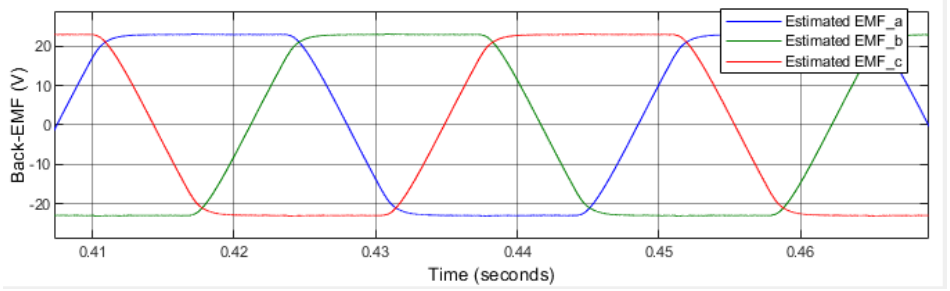

(b)

FIGURE 5.16: Detailed View of Back-EMF Comparison for Observer Performance Analysis a) Ideal Back-EMF Signal (b) Estimated Back-EMF Signal

the standard trapezoidal reference signal but there is a slight phase shift in the estimated signals. As we have used the low pass filter in our design of the observer,

this filtration process can be a reason of the sight phase shift that we have seen. Other than the slight phase shift, SMO has a very good performance in estimating back-EMF. The phase shift issue can be resolved.

We have proposed a very simple and effective design for our sliding mode observer (SMO) in order to keep the implementation as simple and easy as possible. The proposed design can be slightly modified to accommodate the phase shift issue.

5.4.3 Estimated Back-EMF and Current Comparison

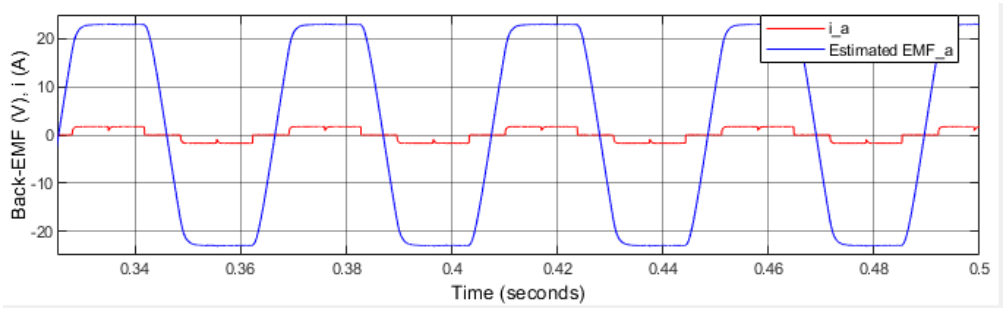

(a)

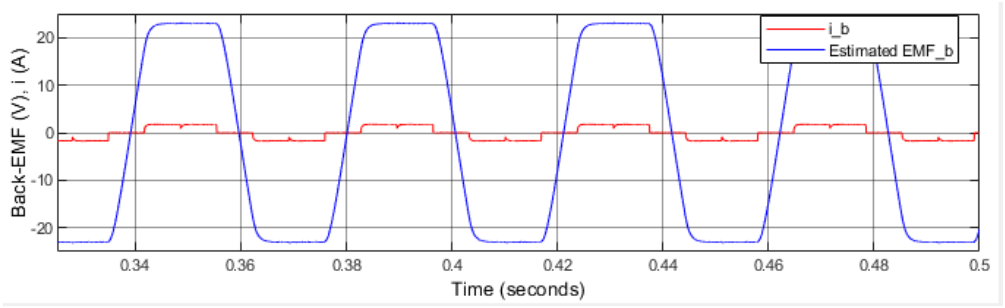

(b)

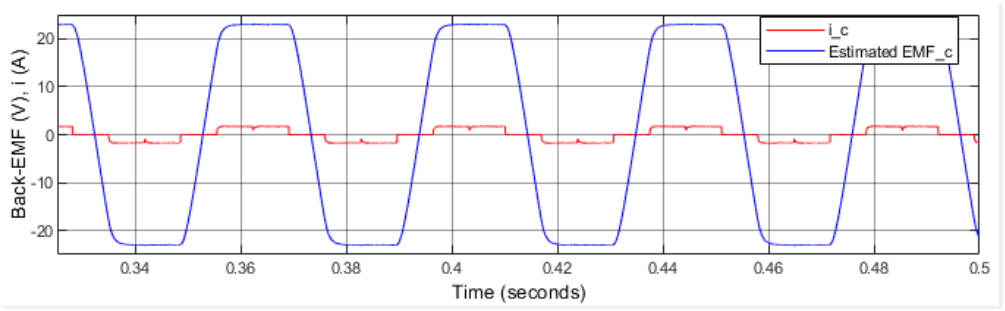

(c)

FIGURE 5.17: Back-EMF Comparison with Phase Current (a) Back-EMF and Current of Phase-A (b) Back-EMF and Current of Phase-B (c) Back-EMF and Current of Phase-C

The sequence of the phase current with its back-EMF is important and needs to be consistent with each other. Fig. 5.17 shows the comparison of phase current and back-EMF of all phases. We can analyze that when the current is positive, the estimated EMF signal is also positive. When the phase current is negative, the estimated EMF is also negative. The estimated EMF signal changes its state from positive peak to negative peak where the input current is also shifted from positive peak to negative peak and vice versa. Here, it is also observed that the zero crossings of the input current and the estimated back-EMF of the respective phase are consistent with each other. If we analyze the figure in detail, we can see that there is point in zero crossing where the current in the stator winding changes its states. At this point the back-EMF of the respective phase also changes its state. When the current is positive, the EMF is positive and vice versa. Another important point here is to discuss that there is phase difference between the currents. These currents were measured from each output terminal of the inverter which is connected to the motor. There is a phase difference in current signals which shows that at each time instant, one phase is connected to positive positive power supply, other is connected to negative terminal of power supply and the remaining phase is not connected.

5.5 Summary

Back-EMF estimation results along with currents are presented in this chapter. Back-EMF of a BLDC motor has a trapezoidal shape. The results of our estimated currents and back-EMFs are compared with previous research in order to check the performance of the observer. The results show that the observer has very good estimation of back-EMF. That result also verify that the algorithm of SMO was efficiently used for estimation. The comparison of the back-EMF with the currents is also presented in order to verify the proper operation of the motor.

Chapter 6

Conclusion and Future Work

Our proposed design involves the estimation of the back-EMF of a three-phase sensorless Brushless DC motor. We have used a sensorless BLDC motor and the back-EMF is estimated using SMO. Back-EMF signal is required to generate the switching signals for the three-phase inverter in order to operate the motor. Sliding mode observer (SMO) is designed using currents of respective phases in order to estimate the back-EMF of three phases of the BLDC motor. The results of the implementation of proposed observer in MATLAB/Simulink are compared with previous research results. As a result of this analysis, it was concluded that the observer has a very good estimation of the back-EMF of the motor. The observer design is very simple and effective as compared to that of previous research which had complex design of observer. There is a slight phase shift in our back-EMF estimation results when compared with a standard reference signal. This phase shift can be removed using effective and easy techniques. We want to design a complete control system of a BLDC motor on hardware in the future. This research will be helpful for estimation purposes.

Bibliography

[1] C.-l. Xia, *"Permanent magnet brushless DC motor drives and controls"*, 1st ed. Singapore: John Wiley & Sons, 2012, ch. 1, pp. 1–8.

[2] P. Yedamale, "Brushless dc (bldc) motor fundamentals," *Microchip Technology Inc*, vol. 20, no. 1, pp. 3–15, 2003.

[3] M. Yılmaz and S. Özdemir, "Review of motors used in commercial electric vehicles," in *5th International Mediterranean Science and Engineering Congress (IMSEC 2020)*, 2020, pp. 585–591.

[4] E. Agamloh, A. Von Jouanne, and A. Yokochi, "An overview of electric machine trends in modern electric vehicles," *Machines*, vol. 8, no. 2, pp. 1–16, 2020.

[5] D. Mohanraj, R. Aruldavid, R. Verma, K. Sathyasekar, A. B. Barnawi, B. Chokkalingam, and L. Mihet-Popa, "A review of bldc motor: State of art, advanced control techniques, and applications," *IEEE Access*, vol. 10, pp. 54 833–54 869, 2022.

[6] T. A. Zarma, A. A. Galadima, and M. A. Aminu, "Review of motors for electric vehicles," *Journal of Scientific Research and Reports*, vol. 24, no. 6, pp. 1–6, 2019.

[7] D.-M. Stănică, N. Bizon, and M.-C. Arva, "A brief review of sensorless motors position control," in *2021 13th International Conference on Electronics, Computers and Artificial Intelligence (ECAI)*. IEEE, 2021, pp. 1–6.

[8] H. Khambhadiya and A. Dhaneria, "Sensorless control method of 3-phase bldc motor through back-emf observer," in *2021 International Conference on Advances in Electrical, Computing, Communication and Sustainable Technologies (ICAECT)*. IEEE, 2021, pp. 1–5.

[9] R. Patil, A. Gaikwad, and D. Patil, "Implementation of position sensorless brushless dc motor drive," in *2018 International Conference on Inventive Research in Computing Applications (ICIRCA)*. IEEE, 2018, pp. 1346–1349.

[10] S. M. Awchar, S. P. Diwan, and P. Arlikar, "Advanced technique for speed control of sensor-less bldc motor," in *2018 Fourth International Conference on Computing Communication Control and Automation (ICCUBEA)*. IEEE, 2018, pp. 1–5.

[11] C. Shrutika, S. Matani, S. Chaudhuri, A. Gupta, S. Gupta, and N. Singh, "Back-emf estimation based sensorless control of brushless dc motor," in *2021 1st International Conference on Power Electronics and Energy (ICPEE)*. IEEE, 2021, pp. 1–6.

[12] A. Y. Alanis, G. Munoz-Gomez, and J. Rivera, "Nested high order sliding mode controller with back-emf sliding mode observer for a brushless direct current motor," *Electronics*, vol. 9, no. 6, pp. 1041–1060, 2020.

[13] M. Topal, I. Iskender, and N. Genc, "Sensorless speed control of a bldc motor using improved sliding mode observer technique," *International Journal on Technical and Physical Problems of Engineering*, vol. 11, no. 1, pp. 1–9, 2019.

[14] O. Sandre-Hernandez, P. Ordaz-Oliver, and C. Cuvas-Castillo, "Sensorless field oriented control of bldc motor based on sliding mode observer," in *2019 International Conference on Mechatronics, Electronics and Automotive Engineering (ICMEAE)*. IEEE, 2019, pp. 119–124.

[15] X. Chen and G. Liu, "Sensorless optimal commutation steady speed control method for a nonideal back-emf bldc motor drive system including buck converter," *IEEE Transactions on Industrial Electronics*, vol. 67, no. 7, pp. 6147–6157, 2019.

[16] B. Alsayid, W. A. Salah, and Y. Alawneh, "Modelling of sensored speed control of bldc motor using matlab/simulink," *International Journal of Electrical and Computer Engineering*, vol. 9, no. 5, pp. 3333–3343, 2019.

[17] K. Sushita and N. Shanmugasundaram, "Performance and comparative analysis of bldc motor with pi and pid controllers," *Annals of the Romanian Society for Cell Biology*, vol. 25, no. 3, pp. 219–228, 2021.

[18] F. D. J. Lionel, J. Jayan, M. K. Srinivasan, and P. Prabhakaran, "Dc-link current based position estimation and speed sensorless control of a bldc motor used for electric vehicle applications," *International Journal of Emerging Electric Power Systems*, vol. 22, no. 3, pp. 269–284, 2021.

[19] M. Mahmud, S. Motakabber, A. Z. Alam, and A. N. Nordin, "Control bldc motor speed using pid controller," *International Journal of Advanced Computer Science and Applications*, vol. 11, no. 3, pp. 477–481, 2020.

[20] M. H. Centre, "What is an S-function?" Accessed Sep. 1, 2022. [Online]. Available: https://www.mathworks.com/help/simulink/sfg/what-is-an-s-function.html

[21] X. Song, B. Han, S. Zheng, and J. Fang, "High-precision sensorless drive for high-speed bldc motors based on the virtual third harmonic back-emf," *IEEE transactions on Power Electronics*, vol. 33, no. 2, pp. 1528–1540, 2017.

[22] I. N. Syamsiana, M.-S. Wang, and A. D. W. Sumari, "A study on sensorless trapezoidal bldc motors based on back-emf zero crossing detection method," in *2019 2nd International Conference on Applied Engineering (ICAE)*. IEEE, 2019, pp. 1–6.